Supporting Information

Substrate sequence controls regioselectivity of lanthionine formation by ProcM

Tung Le,[a,#] Kevin Jeanne Dit Fouque,[b,#] Miguel Santos-Fernandez,[b] Claudio D. Navo,[c] Gonzalo Jiménez-Osés,[c] Raymond Sarksian,[a] Francisco Alberto Fernandez Lima[b,*] and Wilfred A. van der Donk[a,*]

[a]Department of Chemistry and Howard Hughes Medical Institute, University of Illinois at Urbana–Champaign, 600 S. Mathews Ave, Urbana, IL. 61801, USA

[b] Department of Chemistry and Biochemistry, Florida International University, 11200 SW 8th St, Miami, FL 33199, USA.

[c] Center for Cooperative Research in Biosciences (CIC bioGUNE), Basque Research and Technology Alliance (BRTA), Bizkaia Technology Park, Building 800, 48160 Derio, Spain; Ikerbasque, Basque Foundation for Science, 48013 Bilbao, Spain.

[#] These authors contributed equally to this work

*Correspondence: vddonk@illinois.edu (W.A. van der Donk); phone: (217) 244-5360, fax: (217) 244-8533. fernandf@fiu.edu (F. Fernandez-Lima); phone: (305) 348-2037

Materials and methods

General methods and reagents

Oligonucleotides were obtained from Integrated DNA Technologies. Cloning was performed using restriction enzymes, Q5 polymerase and Hifi DNA Assembly (for isothermal assembly) purchased from New England Biolabs (NEB). All polymerase chain reactions were carried out on a C1000 thermal cycler (Bio-Rad). DNA sequencing was performed by ACGT, Inc. MALDI-TOF MS was carried out on a Bruker Daltonics UltrafleXtreme MALDI TOF/TOF instrument (Bruker). LC-ESI-Q/TOF MS (ESI, electrospray ionization; Q: quadrupole) and MS/MS analyses were conducted using a Synapt G1 instrument with an Acquity UPLC system (Waters). To obtain MS/MS data at higher resolution, a second round of LC-MS/MS was performed on the same mutants using an Agilent Infinity1260 LC coupled to an Agilent 6545 LC/QTOF instrument, which are the MS/MS spectra shown. To compare LC and TIMS product ratios, the Extracted Ion Chromatograms (EIC) data in the figures are shown for the first round of samples, as these were the samples that were used for the TIMS.

Strains and plasmids

Unless stated otherwise, *E. coli* DH10B and *E. coli* BL21(DE3)-T1^{R} were used as hosts for cloning and protein expression, respectively. The co-expression vector pRSFDuet-1 was obtained from Novagen.

Construction of the ProcA3.3 library

Plasmid pET15b_procA3.3[1] was used as template for PCR using primers procA3.3_invar_F/R (Table S2) to amplify ProcA3.3 up until the first randomized residue of ProcA3.3 (i.e. including Thr11). The PCR product was gel-purified and inserted between EcoRI and AscI sites of pRSF_procM[2] containing *procM* in multiple cloning site 2 (MCS 2) of pRSFDuet-1 to yield

pRSF_procA3.3invar_procM. About 4 µg of this plasmid was digested with AscI and NotI, followed by gel-purification to yield the backbone for library construction.

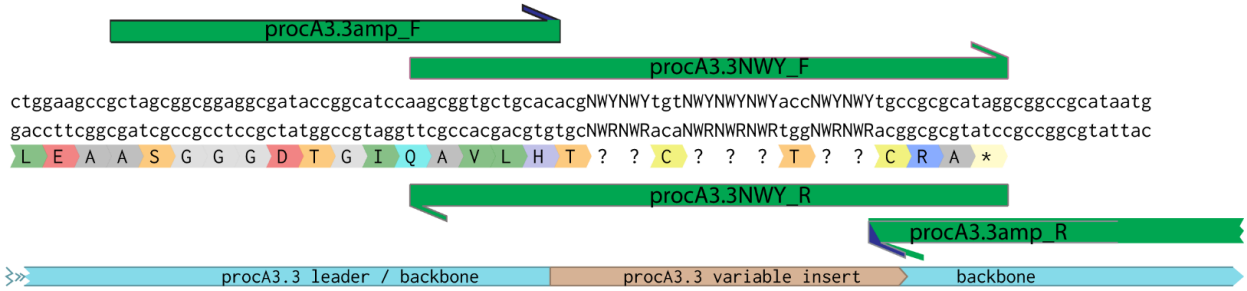

Scheme S1. Cloning scheme for procA3.3 core region containing randomized NWY codons. Primers procA3.3amp_F/R contain homology region with pRSF_procA3.3invar_procM (backbone) for isothermal assembly.

To create inserts containing the randomized core peptide of ProcA3.3, degenerate primers procA3.3NWY_F/R were mixed and amplified with primers procA3.3amp_F/R (Scheme S1), followed by gel-purification. About ~500 ng of this PCR product was combined with ~2 µg of linearized pRSF_procA3.3invar_procM in 20 µL of ddH_2O and assembled by isothermal assembly (NEB Hifi DNA assembly) for 1 h to yield pRSF_procA3.3NWY_procM. The assembly reaction was purified and concentrated using DNA Clean & Concentrator-5 (Zymo Research), and eluted with 10 µL of ddH_2O. The purified DNA was divided into 5 aliquots and used to electroporate 5x25-µL aliquots of 10-beta electrocompetent *E. coli* (NEB). Each aliquot was rescued with 1 mL of Super Optimal broth with Catabolite repression (SOC media: 0.5% (w/v) yeast extract, 2% (w/v) tryptone, 10 mM NaCl, 2.5 mM KCl, 20 mM $MgSO_4$, 0.5% (w/v) glucose). The aliquots were pooled and incubated at 37 ºC for 1 h. Then 5 µL was plated as serial dilution onto LB/kanamycin plate to approximate the library size (10^6 – 10^7 members), while the remaining culture was used to inoculate 50 mL of TB/kanamycin and cultured overnight at 37 ºC, then divided into 5-mL

aliquots. One aliquot was used for miniprep while glycerol was added to the others to 10% and stored at -70 ºC.

LC-ESI-MS/MS of ProcA3.3 variants

LC-ESI MS and MS/MS analyses were performed on an Agilent Infinity1260 LC coupled to an Agilent 6545 LC/QTOF instrument. Separation was performed on a Vydac 214MS C4 column running at 0.4 mL/min. Mobile phases were solvent A (0.1% formic acid in water) and solvent B (0.1% formic acid in acetonitrile). The following gradient was used: 5% B for 3 min, 5-50%B over 10 min. For mass spectrometry, the instrument was set to run in positive mode with mass range 100 – 1700 m/z and the following parameters: gas temperature: 320 ºC; gas flow: 8 L/min, nebulizer: 35 psi; sheath gas temperature: 350 ºC. For MS: VCap: 3500; nozzle voltage: 1000 V; fragmentor: 125 V; skimmer 1: 65. For MS/MS, the instrument was set to run Auto MS2 mode where eight most abundant precursor ions in each survey scan were selected and fragmented at either 20 V or 25 V collision energy. MS/MS spectra were extracted from the $[M+3H]^{3+}$ parent ion for each peptide and analyzed with the Interactive Peptide Spectral Annotator server.[3]

TIMS-MS/MS of ProcA3.3 variants

Ion mobility experiments were performed on a custom built nanoESI-TIMS coupled to an Impact Q-TOF mass spectrometer (Bruker, Billerica, MA).[4] The TIMS unit was controlled using custom software in LabView (National Instruments) synchronized with the MS platform controls.[5] NanoESI emitters were pulled from quartz capillaries (O.D. = 1.0 mm and I.D. = 0.70 mm) using a Sutter Instrument Co. P2000 laser puller (Sutter Instruments, Novato, CA). The general fundamentals of TIMS as well as the calibration procedure have been described previously.[6-9] Peptide sample solutions were loaded in a pulled-tip capillary, housed in a mounted custom built XYZ stage in front of the MS inlet, and sprayed at 950 V via a tungsten wire inserted inside the

nESI emitters. TIMS-MS experiments were carried out using nitrogen (N_2) as buffer gas at room temperature. The gas velocity was kept constant between the funnel entrance (*P1* = 2.6 mbar) and exit (*P2* = 0.8 mbar). An rf voltage of 250 V_{pp} at 880 kHz was applied to all electrodes. A voltage ramp (V_{ramp}) of -120 to -40 V, deflector voltage (V_{def}) of 60 V and base voltage (V_{out}) of 60 V were used for the mobility separations. Collision induced dissociation (CID) experiments were performed in the collision cell located after the TIMS analyzer. The mass-selected $[M+3H]^{3+}$ ions were fragmented using nitrogen as collision gas at a collision energy of 20-30 V. The lanthipeptides were subjected to C_{18} Zip Tip (Millipore, Burlington, MA) purification, resulting in solutions at final concentrations of ~5 µM in 50:50 acetonitrile/water containing 0.1% formic acid. The instrument was externally calibrated using the Tuning Mix (Agilent, Santa Clara, CA).

Molecular Dynamics (MD) simulations

Unconstrained MD simulations were carried out with AMBER 18 package[10] implemented with *ff14SB*[11] and general Amber force field (*gaff2*)[12] force fields. Parameters for non-natural dehydroamino acids and (methyl)lanthionine were generated with the *antechamber* module of AMBER, using *gaff2* force field and with partial charges set to fit the electrostatic potential generated with HF/6-31G(d) using the RESP[13] method. The charges were calculated according to the Merz-Singh-Kollman scheme using Gaussian 16.[14] Each peptide was immersed in a water box with a 10 Å buffer of TIP3P[15] water molecules and neutralized by adding explicit Na^+ or Cl^- counterions. A two-stage geometry optimization approach was performed. The first stage minimizes only the positions of solvent molecules and ions, and the second stage is an unrestrained minimization of all the atoms in the simulation cell. The systems were then heated by incrementing the temperature from 0 to 300 K under a constant pressure of 1 atm and periodic boundary conditions. Harmonic restraints of 10 kcal/mol were applied to the solute, and the Andersen temperature coupling scheme[16,17] was used to control and equalize the temperature. The time step

was kept at 1 fs during the heating stages, allowing potential inhomogeneities to self-adjust. Water molecules were treated with the SHAKE algorithm[18] such that the angle between the hydrogen atoms is kept fixed through the simulations. Long-range electrostatic effects were modelled using the particle mesh Ewald method.[19] An 8 Å cut-off was applied to Lennard-Jones interactions. Each system was equilibrated for 2 ns with a 2 fs time step at a constant volume and temperature of 300 K. Production trajectories were then run for 1.0 μs under the same conditions.

For the calculation of the relative energies of constitutional isomers, a total of 10,000 conformational configurations (1 frame every 100 ps) were extracted from each simulation of each isomer removing the water molecules and the Na^+ or Cl^- counterions. Then, each configuration was minimized with AMBER 18 for a maximum of 5,000 minimization cycles (the steepest descent method is used for the initial 2,500 cycles, then it switches to conjugate gradient), using the Generalized Born (GB) OBC-II continuum solvent model.[20] The lowest energy computed for each isomer was considered in each case.

Table S1. Summary of LC-ESI-MS/MS ring pattern results of tested ProcA3.3 mutants. All mutants are mostly dehydrated at all three available Thr residues.

	Core peptide sequence	Ring pattern	Ratio LC-MS[a]	Ratio TIMS
WT	GDTGIQAVLHT**AG**C**YGG**T**KM**CRA	overlapping	>100:1[b]	>100:1[b]
procA3.3_1	GDTGIQAVLHT**LI**C**FVI**T**HL**CRA	both	<1:100	5:95
procA3.3_2	GDTGIQAVLHT**ID**C**VVI**T**FY**CRA	non-overlapping	<1:100	<1:100
procA3.3_3	GDTGIQAVLHT**DN**C**LVF**T**FV**CRA	non-overlapping	<1:100	<1:100
procA3.3_4	GDTGIQAVLHT**IY**C**NNL**T**VI**CRA	both	20:80	25:75
procA3.3_5	GDTGIQAVLHT**HN**C**VIN**T**FV**CRA	both	40:60	30:70
procA3.3_6	GDTGIQAVLHT**IY**C**ILD**T**HL**CRA	both	45:55	52:48
procA3.3_7	GDTGIQAVLHT**HF**C**NYL**T**YI**CRA	non-overlapping	<1:100	<1:100
procA3.3_8	GDTGIQAVLHT**YN**C**YYY**T**YI**CRA	non-overlapping	<1:100	<1:100
procA3.3_9	GDTGIQAVLHT**IL**C**LIF**T**VD**CRA	both	N.D.	42:58
procA3.3_10	GDTGIQAVLHT**DF**C**LLV**T**HD**CRA	both	N.D.	30:70
procA3.3_11	GDTGIQAVLHT**HF**C**INL**T**YV**CRA	both	75:25	75:25
procA3.3_12	GDTGIQAVLHT**NY**C**NLV**T**HL**CRA	non-overlapping	N.D.	<1:100[c]
procA3.3_13	GDTGIQAVLHT**LF**C**YGG**T**FD**CRA	both	40:60	[d]

[a] The integration ratio is estimated for overlapping/non-overlapping ring patterns. N.D. ratio could not be determined because of co-elution. [b] Estimated detection limit. [c] See Figure S29. [d] Isomers were separated by LC prior to analysis by TIMS. See Figure S30.

Table S2. Primers used for this study

procA3.3_NWY_F	aagcggtgctgcacacgNWYNWYtgtNWYNWYNWYaccNWYNWYtgccgcgcatagtcga
procA3.3_NWY_R	tcgactatgcgcggcaRWNRWNggtRWNRWNRWNacaRWNRWNcgtgtgcagcaccgctt
proc3.3amp_F	cggaggcgataccggcatccaagcggtgctgcacac
proc3.3amp_R	actttctgttcgacttaagcattatgcggccgcctatgcgcggc
procA3.3invar_F	caggatccgaattcggctcggcgcgccatgtcagaagaacaactcaaggc
procA3.3invar_R	ttatgcggccgcaagcttgtcgacctgcaggtgcagcaccgcttggat

Figure S1. Deep sequencing analysis of the ProcA3.3 library. The distribution of the number of times amino acid sequences were identified in the library.

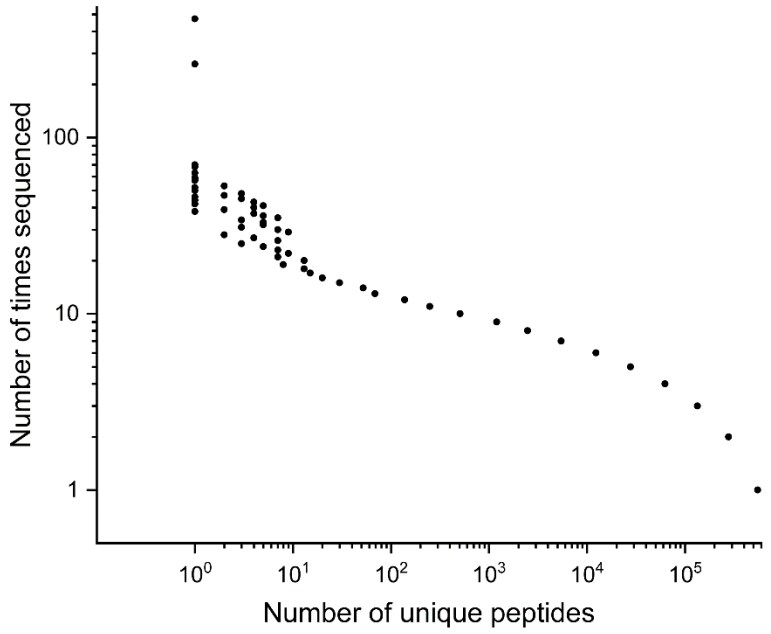

Figure S2. LC-ESI-MS/MS analysis of ProcA3.3_2. (Top) extracted ion chromatogram (EIC) for the selected parent ion $[M+3H]^{3+}$; product with non-overlapping rings is shown in red. (Middle) MS/MS spectrum with b- (blue) and y- (red) ion fragments. For clarity these peaks are boldened and colored. The height of the colored blue and red ions reflects the intensity of the ion; sometimes a grey ion appears to be within the bolded (widened) red and blue peaks; these correspond to the isotopic peaks of the matched fragments. (Bottom) list of matched fragment ions showing theoretical masses, charge states, and mass error (ppm).

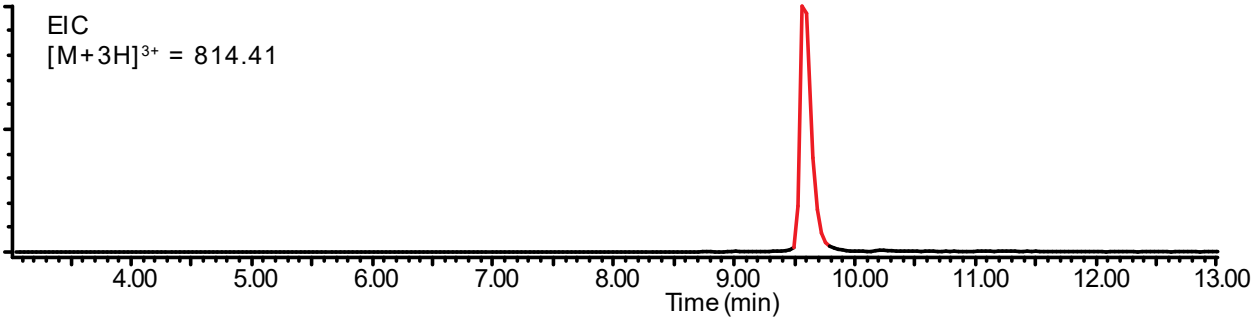

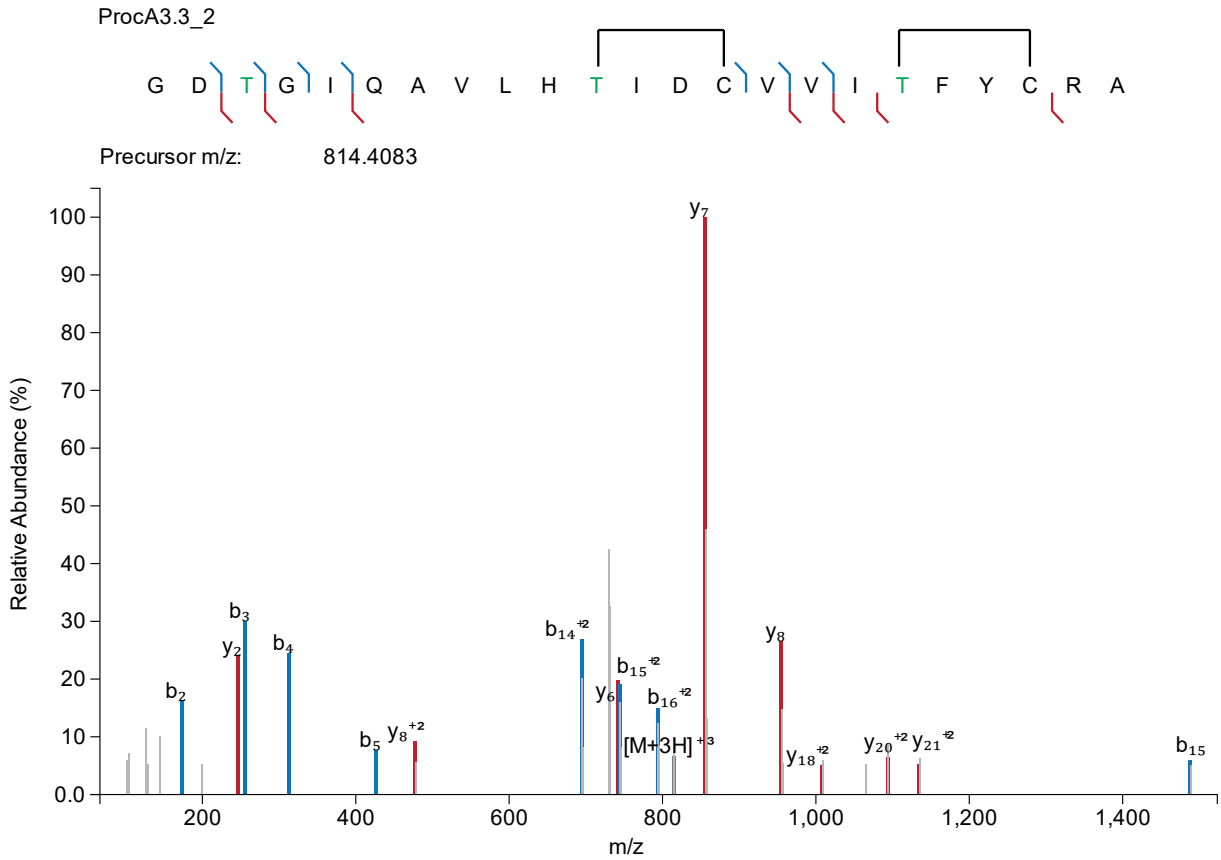

ion	charge	Observed mass	Theoretical mass	Error (ppm)
b2	1	173.0555	173.0557	-1.0168
y2	1	246.156	246.1561	-0.4425
b3	1	256.0925	256.0928	-1.2712
b4	1	313.1138	313.1143	-1.44
b5	1	426.1976	426.1983	-1.5946
y8	2	477.7471	477.7469	0.2884
b14	2	694.8343	694.835	-0.9534

y6	1	742.3326	742.3341	-2.0952
b15	2	744.3682	744.3692	-1.287
b16	2	793.9017	793.9034	-2.1494
M+3H	3	814.4082	814.4083	-0.1997
y7	1	855.4169	855.4182	-1.4623
y8	1	954.4854	954.4866	-1.2456
y18	2	1008.5128	1008.5133	-0.5629
y20	2	1093.5657	1093.5661	-0.3968
y21	2	1135.0845	1135.0846	-0.1679
b15	1	1487.7327	1487.7311	1.0576

Figure S3. LC-ESI-MS/MS analysis of ProcA3.3_3 modified by ProcM. (Top) extracted ion chromatogram (EIC) for the selected parent ion $[M+3H]^{3+}$; product with non-overlapping rings is shown in red. (Middle) MS/MS spectrum with b- (blue) and y- (red) ion fragments. For clarity these peaks are boldened and colored. The height of the colored blue and red ions reflects the intensity of the ion; sometimes a grey ion appears to be within the bolded (widened) red and blue peaks; these correspond to the isotopic peaks of the matched fragments. (Bottom) list of matched fragment ions showing theoretical masses, charge states, and mass error (ppm).

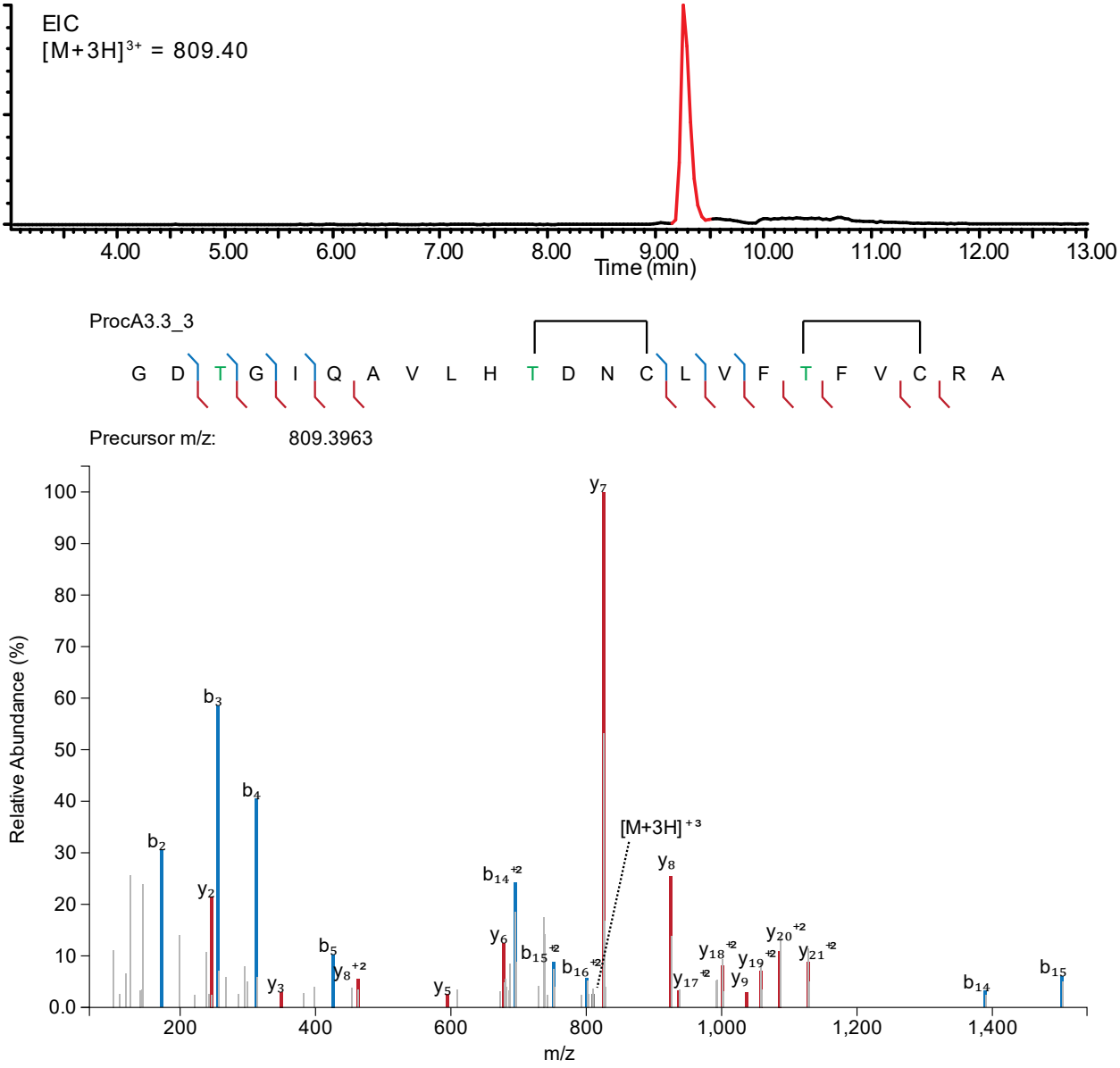

ion	charge	Observed mass	Theoretical mass	Error (ppm)
b2	1	173.0549	173.0557	-4.5099
y2	1	246.1552	246.1561	-3.5146
b3	1	256.0921	256.0928	-2.7169
b4	1	313.1135	313.1143	-2.4265
y3	1	349.1644	349.1653	-2.4491
b5	1	426.1974	426.1983	-2.1581

y8	2	462.7409	462.7416	-1.6153
y5	1	595.2972	595.3021	-8.1961
y6	1	678.3387	678.3392	-0.7289
b14	2	695.3141	695.3144	-0.4671
b15	2	751.8566	751.8565	0.1931
b16	2	801.3907	801.3907	0.0477
M+3H	3	809.3969	809.3963	0.7297
y7	1	825.4085	825.4076	1.085
y8	1	924.4761	924.476	0.0882
y17	2	936.966	936.966	-0.0151
y18	2	1000.995	1000.995	-0.0041
y9	1	1037.56	1037.56	-0.5575
y19	2	1057.538	1057.537	0.346
y20	2	1086.049	1086.048	0.6757
y21	2	1127.568	1127.567	0.8658
b14	1	1389.622	1389.622	0.5231
b15	1	1502.707	1502.706	0.7765

Figure S4. LC-ESI-MS/MS analysis of ProcA3.3_4 modified by ProcM. (Top) extracted ion chromatogram for the selected parent ion $[M+3H]^{3+}$; product with overlapping rings is shown in blue and product with non-overlapping rings is shown in red; (Middle) MS/MS spectrum with b- (blue) and y- (red) ion fragments. For clarity these peaks are boldened and colored. The height of the colored blue and red ions reflects the intensity of the ion; sometimes a grey ion appears to be within the bolded (widened) red and blue peaks; these correspond to the isotopic peaks of the matched fragments. (Bottom) list of matched fragment ions showing theoretical masses, charge states, and mass error (ppm).

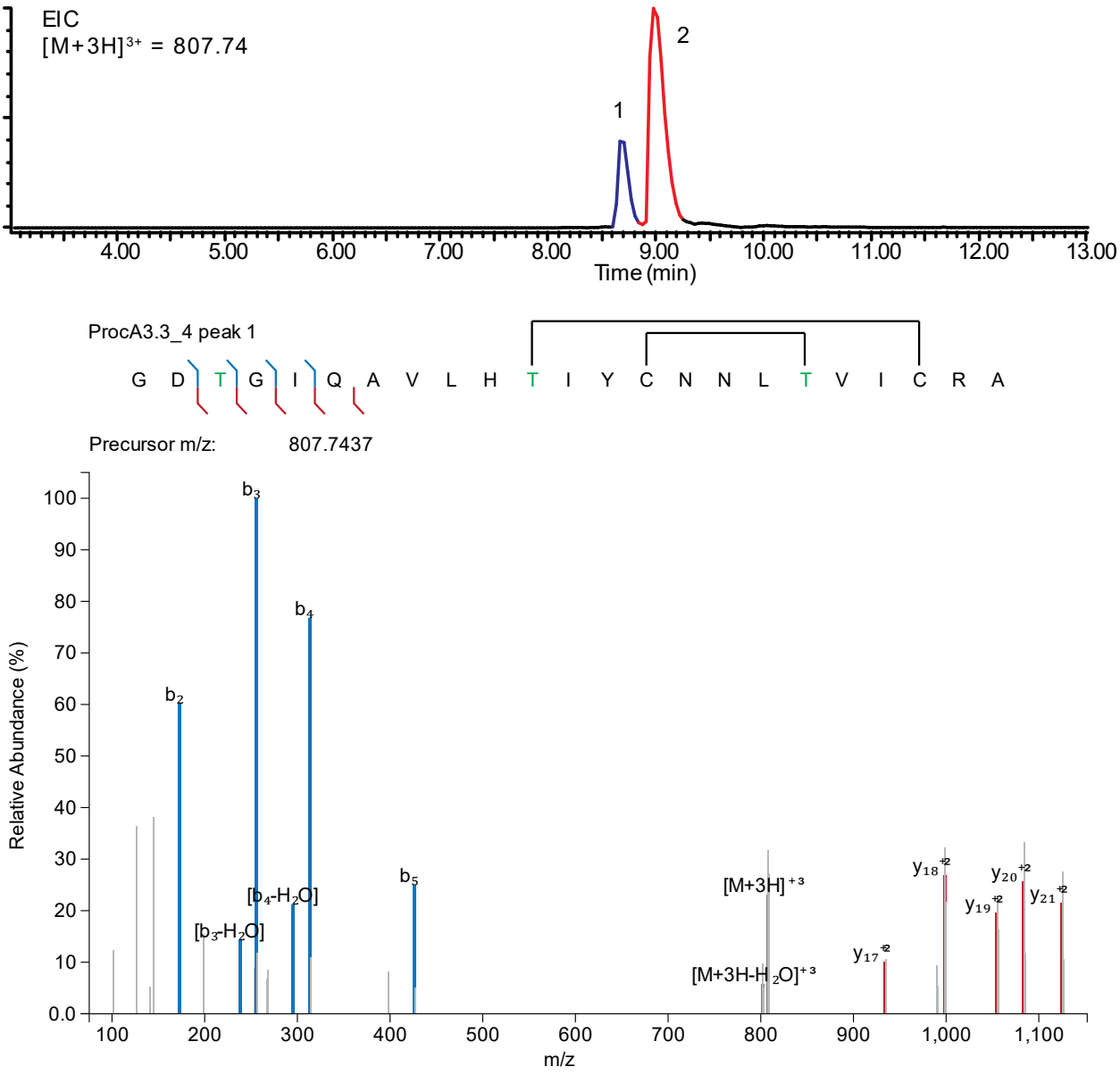

ion	charge	Observed mass	Theoretical mass	Error (ppm)
b2	1	173.0556	173.0557	-0.2895
b3	1	238.0821	238.0822	-0.4611
b3	1	256.093	256.0928	0.6627
b4	1	295.1037	295.1037	0.0754
b4	1	313.1144	313.1143	0.3939

b5	1	426.1981	426.1983	-0.574
M+3H	3	801.7405	801.7402	0.3588
M+3H	3	807.7439	807.7437	0.2698
y17	2	934.4867	934.4871	-0.4092
y18	2	998.5162	998.5164	-0.2019
y19	2	1055.0583	1055.0584	-0.1453
y20	2	1083.5693	1083.5692	0.1333
y21	2	1125.0879	1125.0877	0.1618

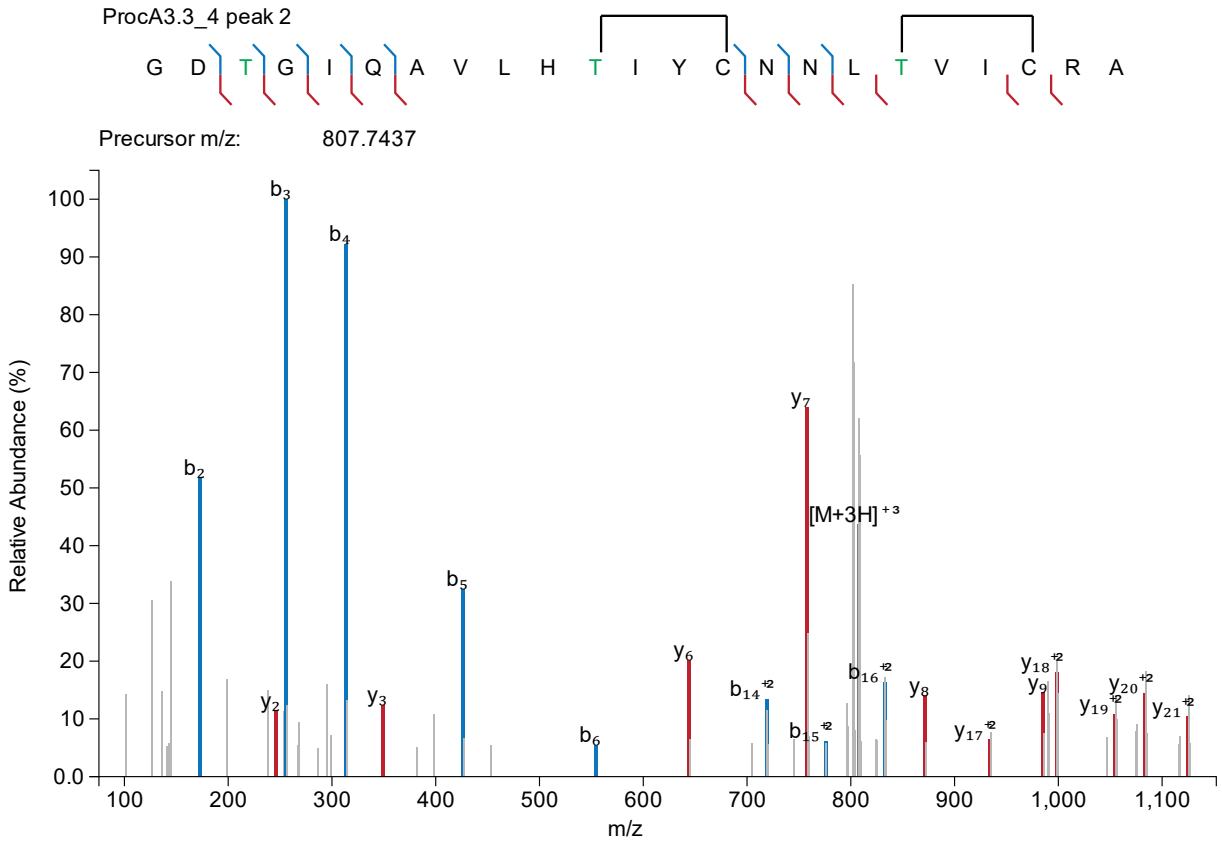

ion	charge	Observed mass	Theoretical mass	Error (ppm)
b2	1	173.0553	173.0557	-2.1763
y2	1	246.1561	246.1561	-0.0507
b3	1	256.0929	256.0928	0.5706
b4	1	313.1146	313.1143	1.0261
y3	1	349.1654	349.1653	0.426
b5	1	426.1984	426.1983	0.1204
b6	1	554.2567	554.2569	-0.3895
y6	1	644.3545	644.3548	-0.4723
b14	2	718.8531	718.8532	-0.0624
y7	1	757.439	757.4389	0.0619
b15	2	775.8747	775.8746	0.0862

M+3H	3	807.7448	807.7437	1.3125
b16	2	832.8961	832.8961	0.039
y8	1	871.4814	871.4818	-0.4622
y17	2	934.4867	934.4871	-0.4305
y9	1	985.5242	985.5248	-0.5447
y18	2	998.5161	998.5164	-0.2806
y19	2	1055.0586	1055.0584	0.1905
y20	2	1083.5694	1083.5692	0.2396
y21	2	1125.088	1125.0877	0.2076

Figure S5. LC-ESI-MS/MS analysis of ProcA3.3_5 modified by ProcM. (Top) extracted ion chromatogram for the selected parent ion $[M+3H]^{3+}$; product with overlapping rings is shown in blue and product with non-overlapping rings is shown in red; (Middle) MS/MS spectrum with b- (blue) and y- (red) ion fragments. For clarity these peaks are boldened and colored. The height of the colored blue and red ions reflects the intensity of the ion; sometimes a grey ion appears to be within the bolded (widened) red and blue peaks; these correspond to the isotopic peaks of the matched fragments. (Bottom) list of matched fragment ions showing theoretical masses, charge states, and mass error (ppm).

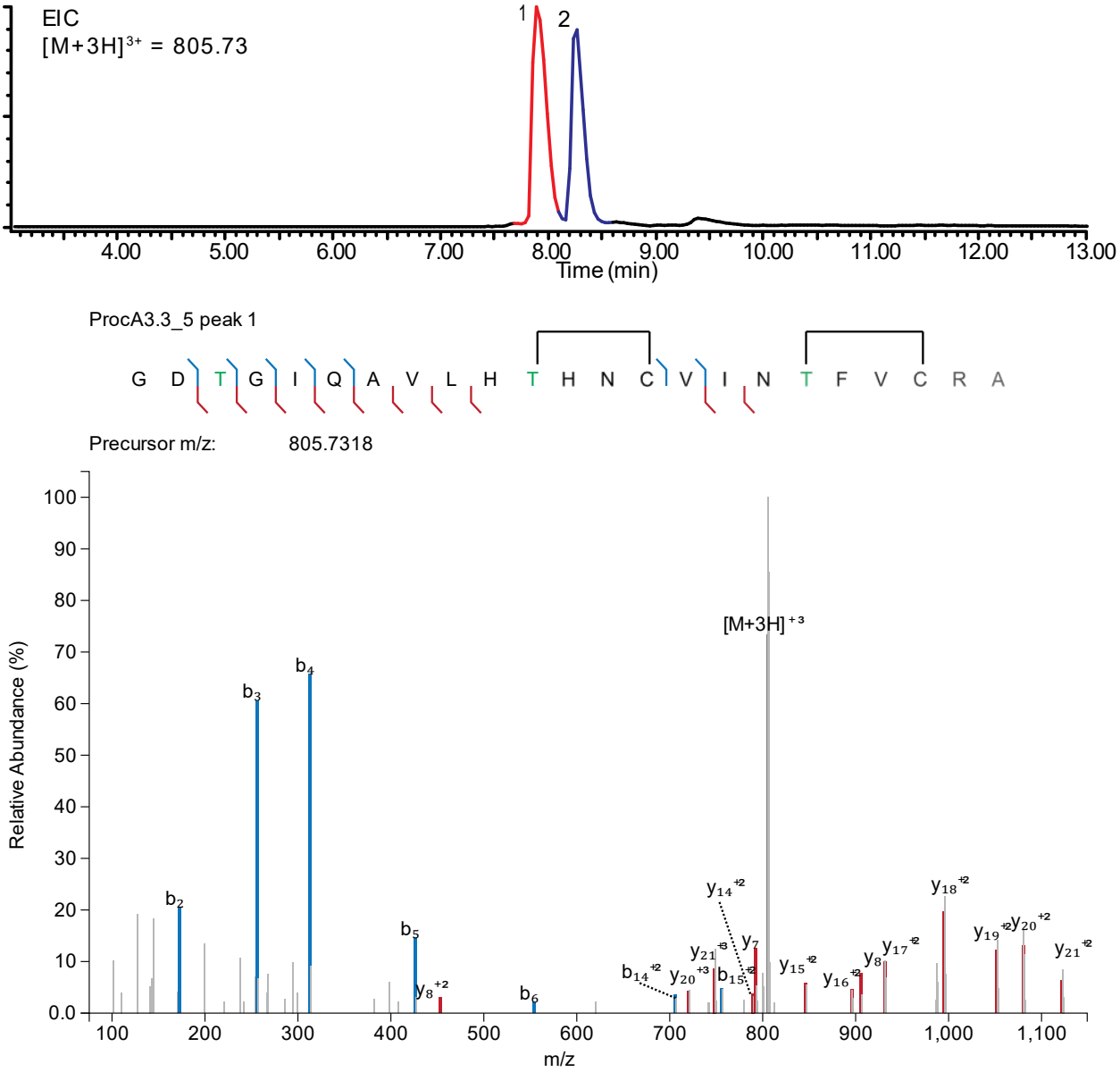

ion	charge	Observed mass	Theoretical mass	Error (ppm)
b2	1	173.0559	173.0557	1.2686
b3	1	256.093	256.0928	0.7974
b4	1	313.1145	313.1143	0.7672
b5	1	426.1981	426.1983	-0.5157
y8	2	453.2446	453.2367	17.363
b6	1	554.2565	554.2569	-0.7213
b14	2	706.3304	706.3304	-0.0139
y20	3	720.7029	720.7033	-0.5544
y21	3	748.3822	748.3823	-0.1844
b15	2	755.8639	755.8646	-0.9483
y14	2	789.8733	789.8745	-1.4751
y7	1	792.3811	792.3821	-1.2929
M+3H	3	805.7322	805.7318	0.489
y15	2	846.4149	846.4165	-1.8846
y16	2	895.9498	895.9507	-1.0069
y8	1	905.4654	905.4662	-0.8664
y17	2	931.4687	931.4693	-0.6003
y18	2	995.4976	995.4985	-0.9534
y19	2	1052.0393	1052.0406	-1.2159
y20	2	1080.5502	1080.5513	-1.0283
y21	2	1122.0693	1122.0699	-0.5069

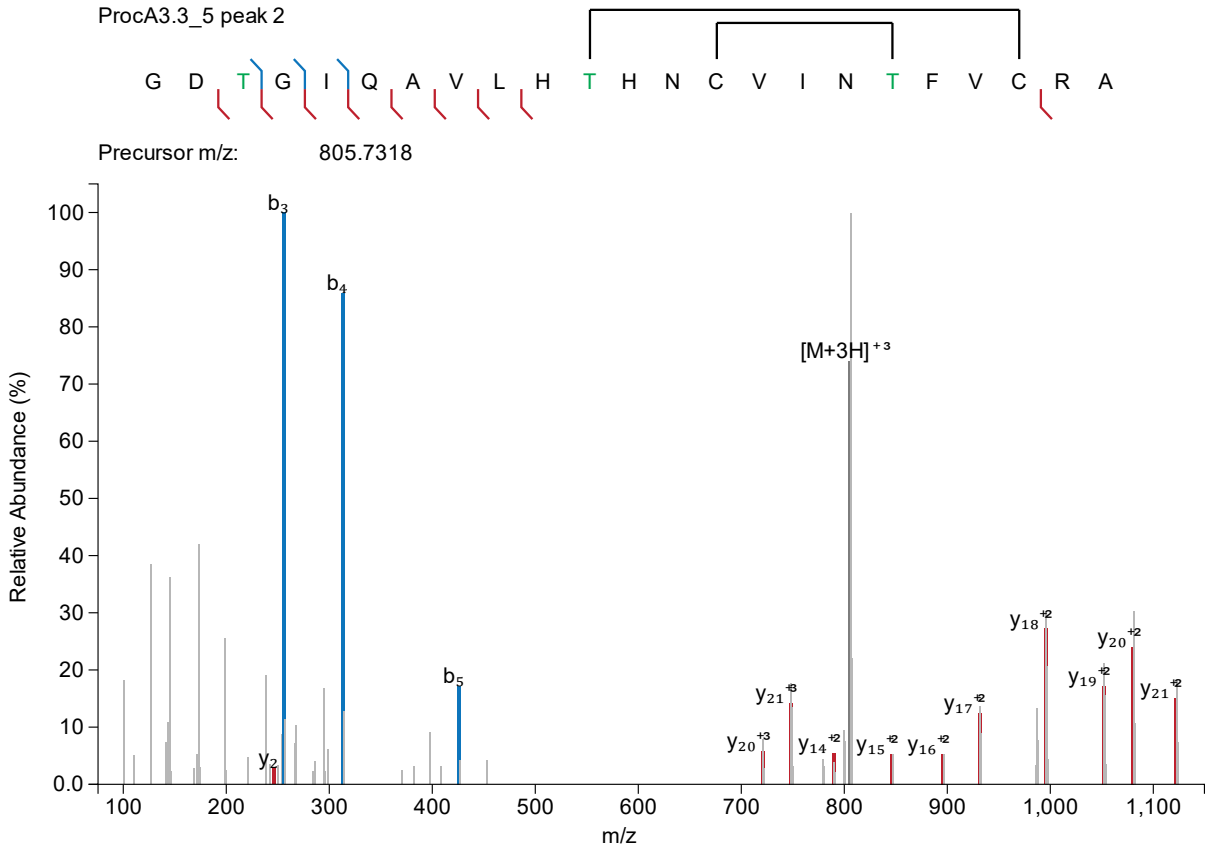

ion	charge	Observed mass	Theoretical mass	Error (ppm)
y2	1	246.1604	246.1561	17.6102
b3	1	256.0971	256.0928	16.8073
b4	1	313.118	313.1143	11.9452
b5	1	426.2004	426.1983	4.8809
y20	3	720.7004	720.7033	-4.0233
y21	3	748.3791	748.3823	-4.3267
y14	2	789.8696	789.8745	-6.1594
M+3H	3	805.7283	805.7318	-4.3513
y15	2	846.4107	846.4165	-6.8467
y16	2	895.9447	895.9507	-6.6992
y17	2	931.4619	931.4693	-7.9006
y18	2	995.4902	995.4985	-8.3869
y19	2	1052.031	1052.041	-8.9152
y20	2	1080.541	1080.551	-9.7276
y21	2	1122.059	1122.07	-9.8646

Figure S6. LC-ESI-MS/MS analysis of ProcA3.3_6 modified by ProcM. (Top) extracted ion chromatogram for the selected parent ion $[M+3H]^{3+}$; product with overlapping rings is shown in blue and product with non-overlapping rings is shown in red; (Middle) MS/MS spectrum with b- (blue) and y- (red) ion fragments. For clarity these peaks are boldened and colored. The height of the colored blue and red ions reflects the intensity of the ion; sometimes a grey ion appears to be within the bolded (widened) red and blue peaks; these correspond to the isotopic peaks of the matched fragments. (Bottom) list of matched fragment ions showing theoretical masses, charge states, and mass error (ppm).

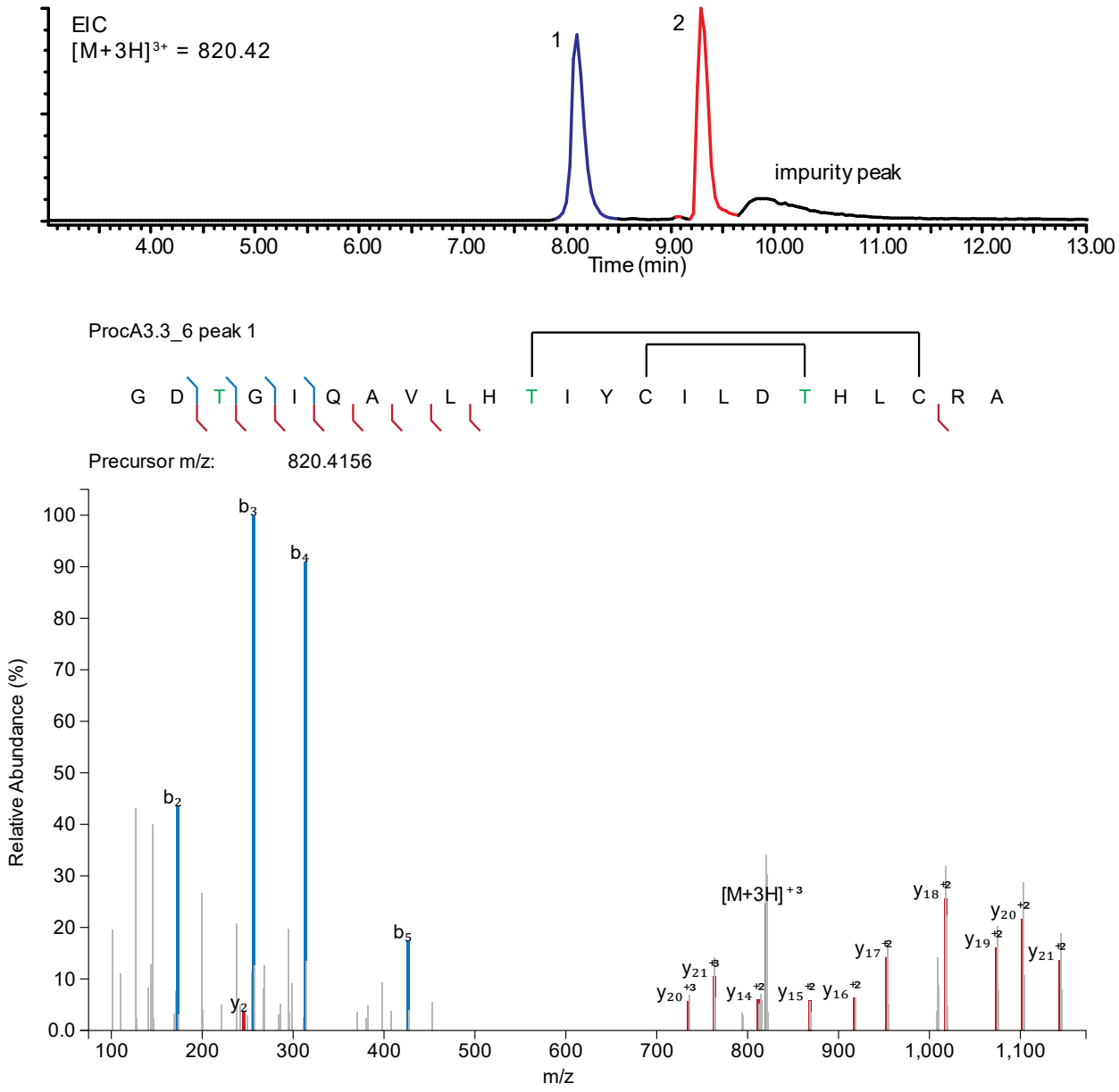

ion	charge	Observed mass	Theoretical mass	Error (ppm)
b2	1	173.0557	173.0557	0.1129
y2	1	246.1559	246.1561	-0.6709
b3	1	256.0928	256.0928	0.0165
b4	1	313.1142	313.1143	-0.1909

b5	1	426.1978	426.1983	-1.2196
y20	3	735.3856	735.3871	-2.0174
y21	3	763.0645	763.0661	-2.1256
y14	2	811.8981	811.9001	-2.514
M+3H	3	820.4143	820.4156	-1.5724
y15	2	868.4397	868.4422	-2.8455
y16	2	917.9735	917.9764	-3.1353
y17	2	953.4922	953.4949	-2.8685
y18	2	1017.522	1017.524	-2.6782
y19	2	1074.064	1074.066	-2.3789
y20	2	1102.574	1102.577	-2.5278
y21	2	1144.093	1144.096	-2.3117

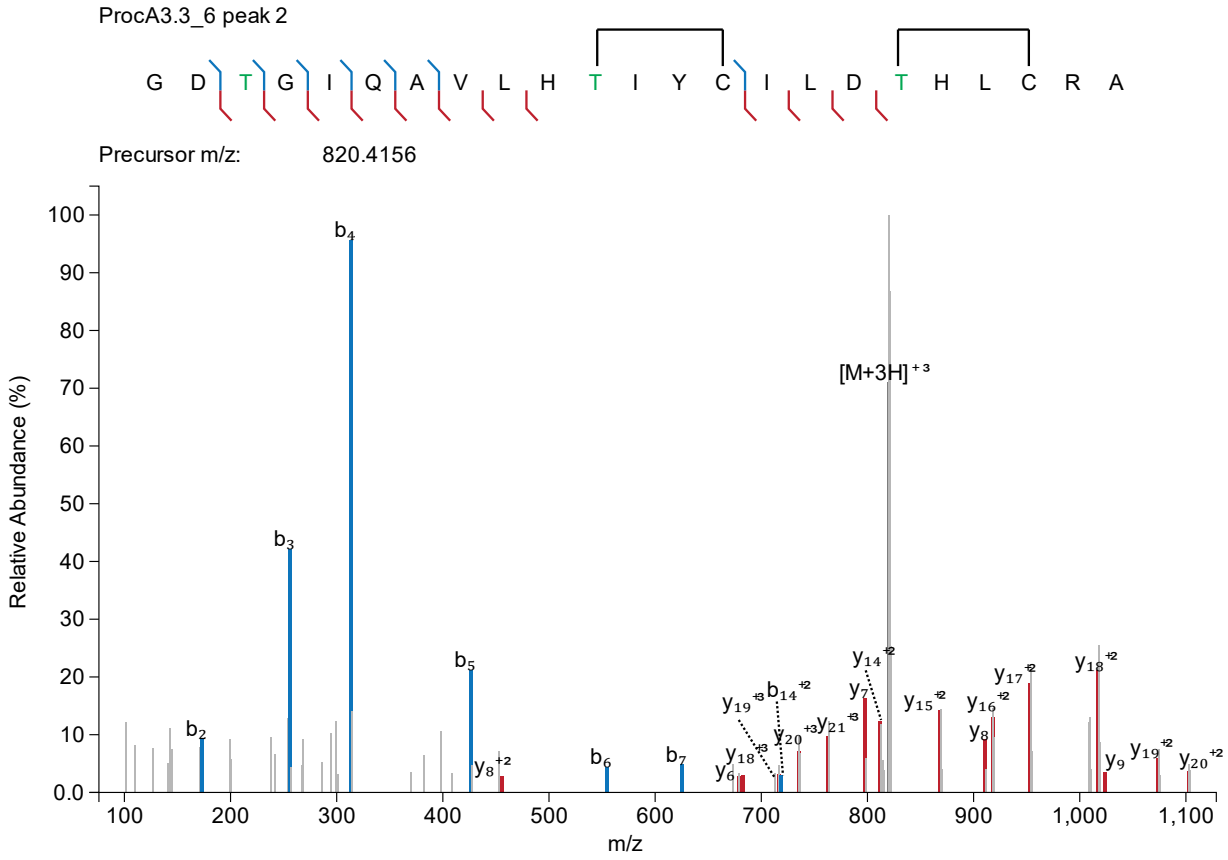

ion	charge	Observed mass	Theoretical mass	Error (ppm)
b2	1	173.0554	173.0557	-1.6207
b3	1	256.0918	256.0928	-3.8884
b4	1	313.113	313.1143	-4.0234
b5	1	426.1956	426.1983	-6.3815
y8	2	455.729	455.7318	-6.1625
b6	1	554.2523	554.2569	-8.299
b7	1	625.2889	625.294	-8.1782
y18	3	678.6796	678.6852	-8.3135
y6	1	682.3387	682.3453	-9.7318

y19	3	716.3734	716.3799	-9.1137
b14	2	718.847	718.8532	-8.6037
y20	3	735.381	735.3871	-8.2726
y21	3	763.0595	763.0661	-8.6782
y7	1	797.3648	797.3723	-9.3814
y14	2	811.8923	811.9001	-9.6577
M+3H	3	820.409	820.4156	-8.0325
y15	2	868.4342	868.4422	-9.1786
y8	1	910.4475	910.4563	-9.7099
y16	2	917.9679	917.9764	-9.2357
y17	2	953.4859	953.4949	-9.4758
y18	2	1017.514	1017.524	-9.8525
y9	1	1023.529	1023.54	-10.8452
y19	2	1074.055	1074.066	-10.1066
y20	2	1074.055	1074.066	-10.1066

Figure S7. LC-ESI-MS/MS analysis of ProcA3.3_7 modified by ProcM. (Top) extracted ion chromatogram (EIC) for the selected parent ion $[M+3H]^{3+}$; product with non-overlapping rings is shown in red. (Middle) MS/MS spectrum with b- (blue) and y- (red) ion fragments. For clarity these peaks are boldened and colored. The height of the colored blue and red ions reflects the intensity of the ion; sometimes a grey ion appears to be within the bolded (widened) red and blue peaks; these correspond to the isotopic peaks of the matched fragments. (Bottom) list of matched fragment ions showing theoretical masses, charge states, and mass error (ppm).

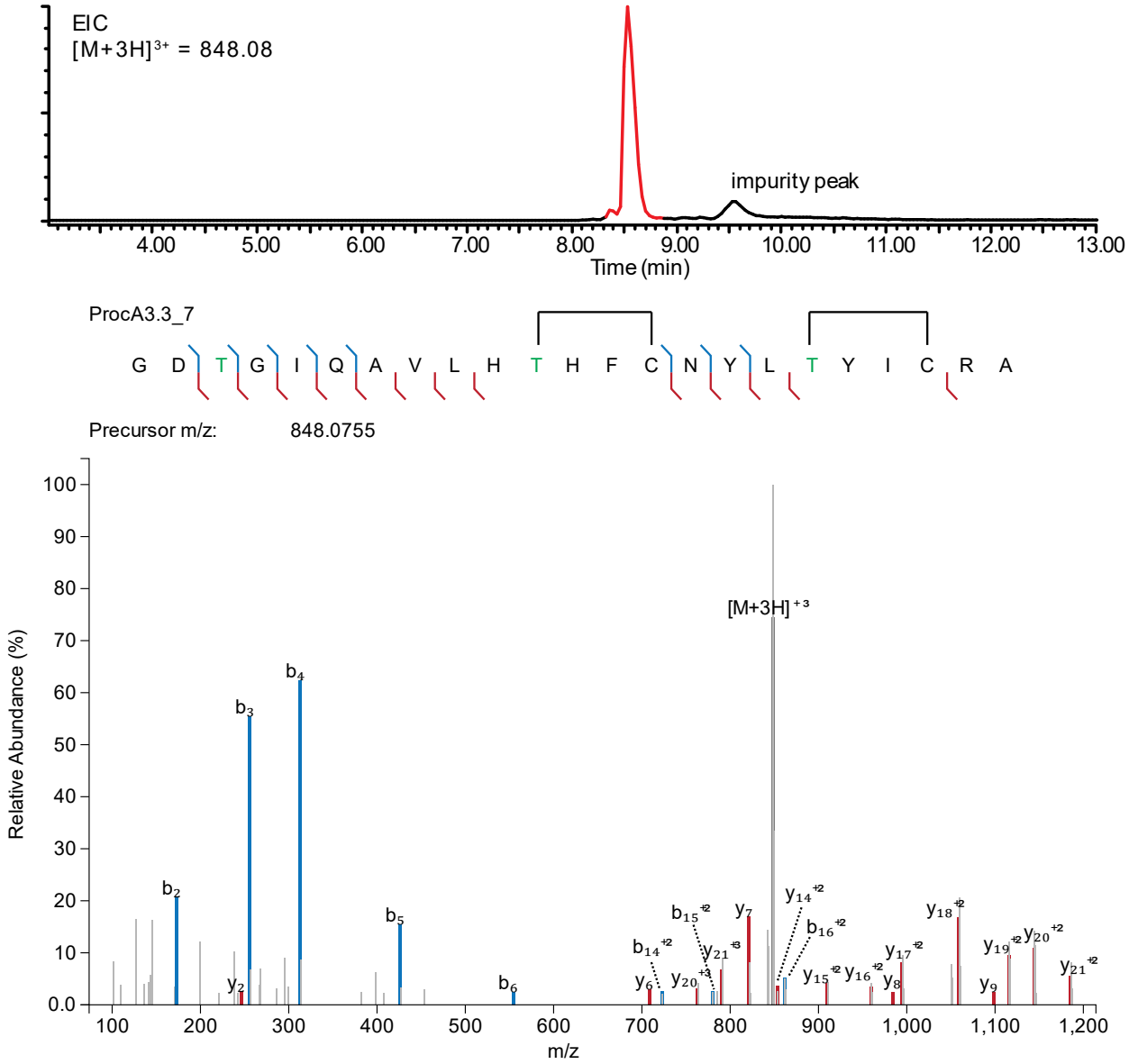

ion	charge	Observed mass	Theoretical mass	Error (ppm)
b2	1	173.0559	173.0557	1.2686
y2	1	246.1564	246.1561	1.3603
b3	1	256.0933	256.0928	1.9689
b4	1	313.1148	313.1143	1.7253
b5	1	426.1987	426.1983	0.8921
b6	1	554.2567	554.2569	-0.3605
y6	1	708.3503	708.3498	0.7617

b14	2	722.8438	722.8431	0.8995
y20	3	763.0474	763.047	0.5851
b15	2	779.8657	779.8646	1.3915
y21	3	790.7269	790.726	1.1483
y7	1	821.4343	821.4338	0.5838
M+3H	3	848.078	848.0755	2.995
y14	2	853.3898	853.3899	-0.1712
b16	2	861.3967	861.3963	0.4878
y15	2	909.9322	909.932	0.246
y16	2	959.4665	959.4662	0.3303
y8	1	984.4978	984.4972	0.6598
y17	2	994.9856	994.9847	0.8642
y18	2	1059.015	1059.014	0.9158
y9	1	1098.54	1098.54	0.1088
y19	2	1115.557	1115.556	0.9322
y20	2	1144.068	1144.067	0.9684
y21	2	1144.068	1144.067	0.9684

Figure S8. LC-ESI-MS/MS analysis of ProcA3.3_8 modified by ProcM. (top) extracted ion chromatogram for the selected parent ion $[M+3H]^{3+}$; product with non-overlapping rings is shown in red; (middle) MS/MS spectrum with b- (blue) and y- (red) ion fragments. (bottom) list of matched fragment ions showing theoretical masses, charge states, and mass error (ppm).

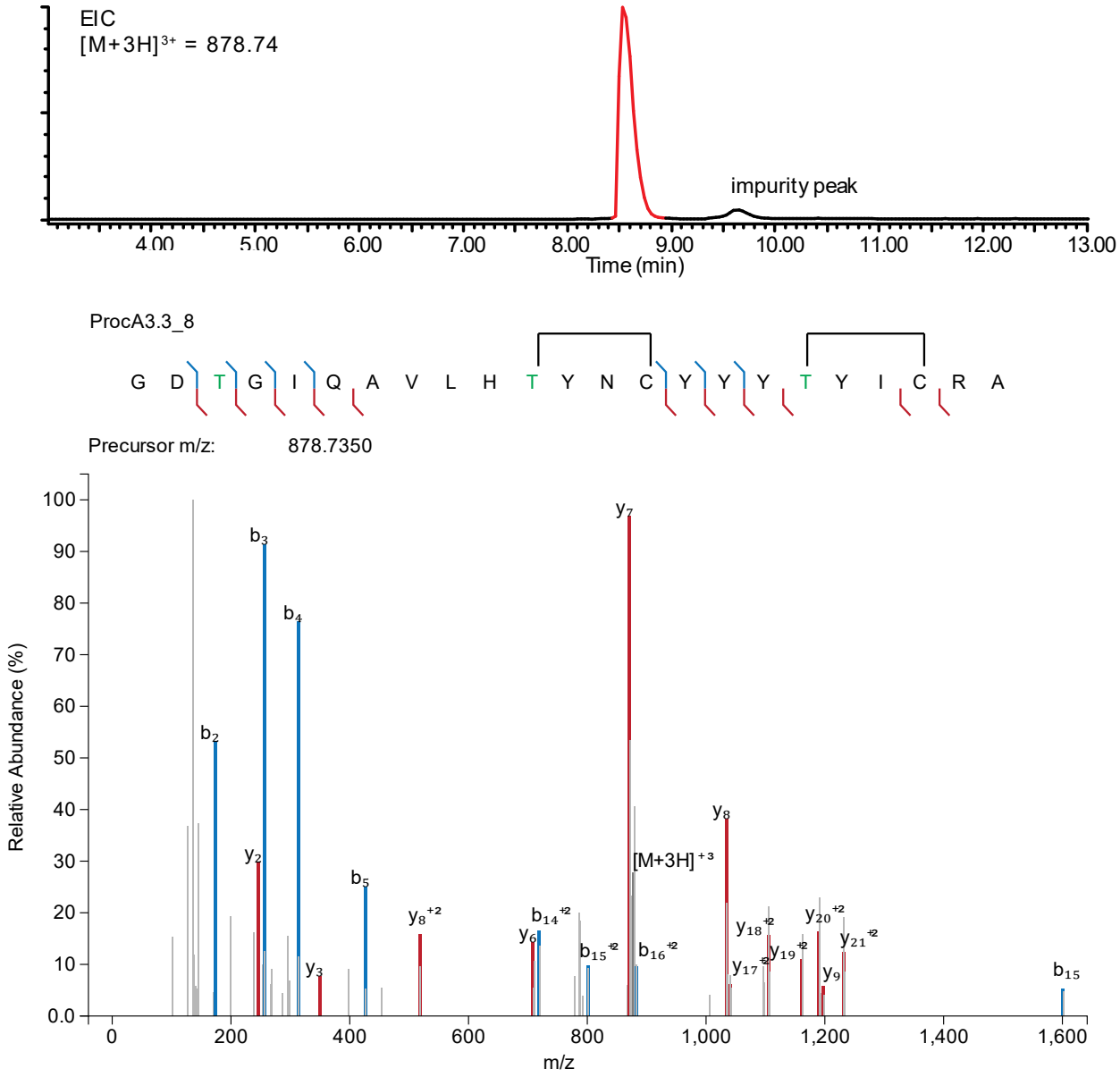

ion	charge	Observed mass	Theoretical mass	Error (ppm)
b2	1	173.0558	173.0557	0.6907
y2	1	246.1562	246.1561	0.5478
b3	1	256.0933	256.0928	1.9689
b4	1	313.1147	313.1143	1.4059
y3	1	349.1651	349.1653	-0.4443
b5	1	426.1983	426.1983	-0.0464
y8	2	517.7419	517.7418	0.0995
y6	1	708.3496	708.3498	-0.2265
b14	2	719.3328	719.3326	0.2505

b15	2	800.8642	800.8643	-0.1059
y7	1	871.4147	871.4131	1.847
M+3H	3	878.7364	878.735	1.597
b16	2	882.3961	882.3959	0.1702
y8	1	1034.477	1034.476	0.7536
y17	2	1040.975	1040.974	0.437
y18	2	1105.004	1105.003	0.9637
y19	2	1161.547	1161.545	0.977
y20	2	1190.057	1190.056	0.9267
y9	1	1197.54	1197.54	0.3754
y21	2	1231.576	1231.575	0.9299
b15	1	1600.722	1600.721	0.4416

Figure S9. LC-ESI-MS/MS analysis of ProcA3.3_9 modified by ProcM. (top) extracted ion chromatogram for the selected parent ion $[M+3H]^{3+}$; (middle) MS/MS spectrum with b- (blue) and y- (red) ion fragments; (bottom) list of matched fragment ions showing theoretical masses, charge states, and mass error (ppm).

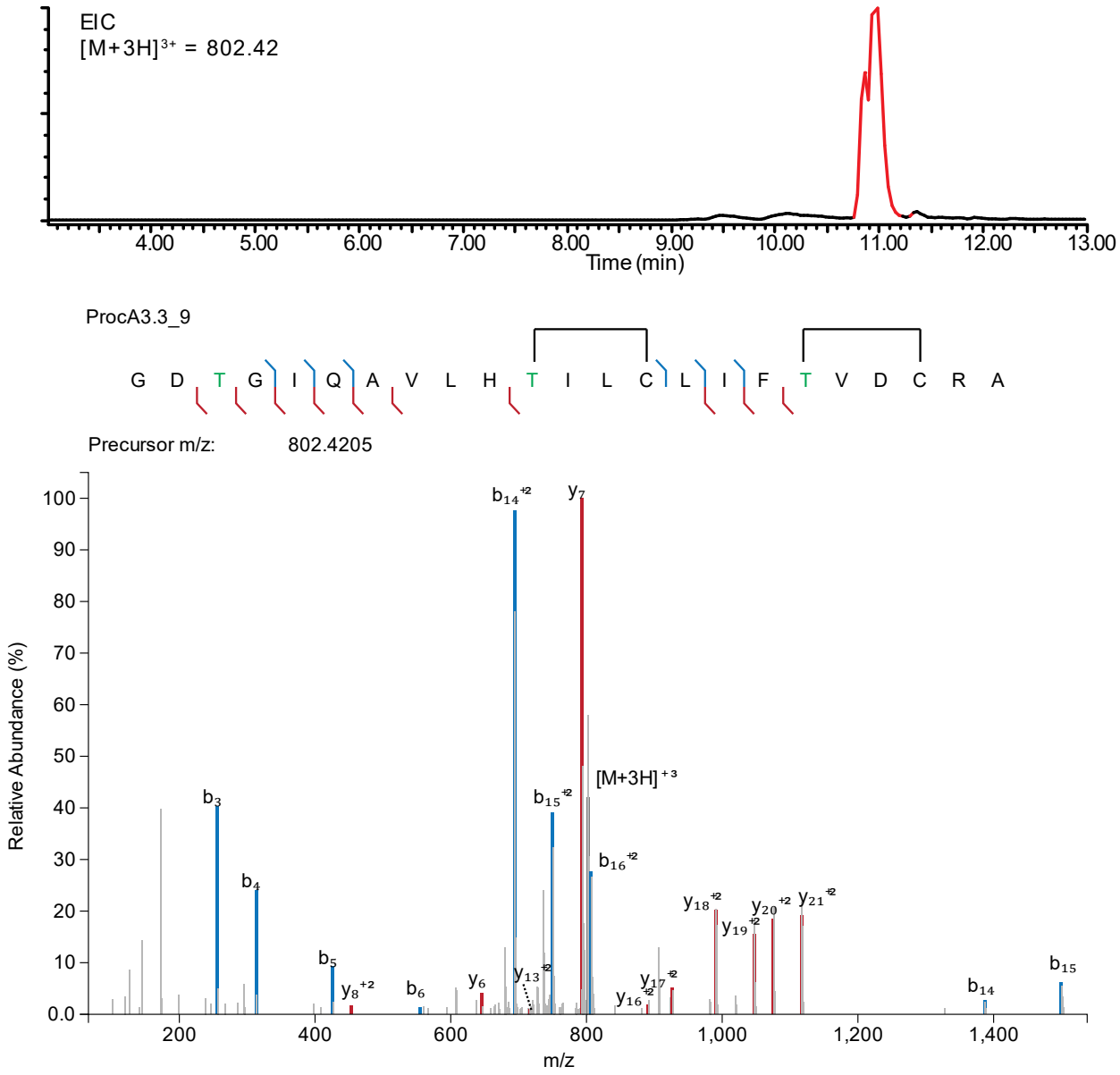

ion	charge	Observed mass	Theoretical mass	Error (ppm)
b3	1	256.0905	256.0928	-8.924
b4	1	313.1135	313.1143	-2.5271
b5	1	426.1998	426.1983	3.4862
y8	2	453.7282	453.7287	-1.1976
b6	1	554.2609	554.2569	7.2153
y6	1	646.3068	646.2977	13.9806
b14	2	693.8617	693.8635	-2.7293
y13	2	716.3757	716.378	-3.1454
b15	2	750.4041	750.4056	-1.9694

y7	1	793.3725	793.3661	7.9725
M+3H	3	802.413	802.4205	-9.2612
b16	2	806.9528	806.9476	6.377
y16	2	890.9796	890.9837	-4.6057
y17	2	926.4964	926.5022	-6.339
y18	2	990.5345	990.5315	2.9917
y19	2	1047.077	1047.074	2.781
y20	2	1075.586	1075.584	1.6864
y21	2	1117.103	1117.103	-0.3185
b14	1	1386.718	1386.72	-1.6846
b15	1	1499.806	1499.804	1.1841

Figure S10. LC-ESI-MS/MS analysis of ProcA3.3_10 modified by ProcM. (Top) Extracted ion chromatogram for the selected parent ion $[M+3H]^{3+}$. (Middle) MS/MS spectrum with b- (blue) and y- (red) ion fragments. (Bottom) list of matched fragment ions showing theoretical masses, charge states, and mass error (ppm).

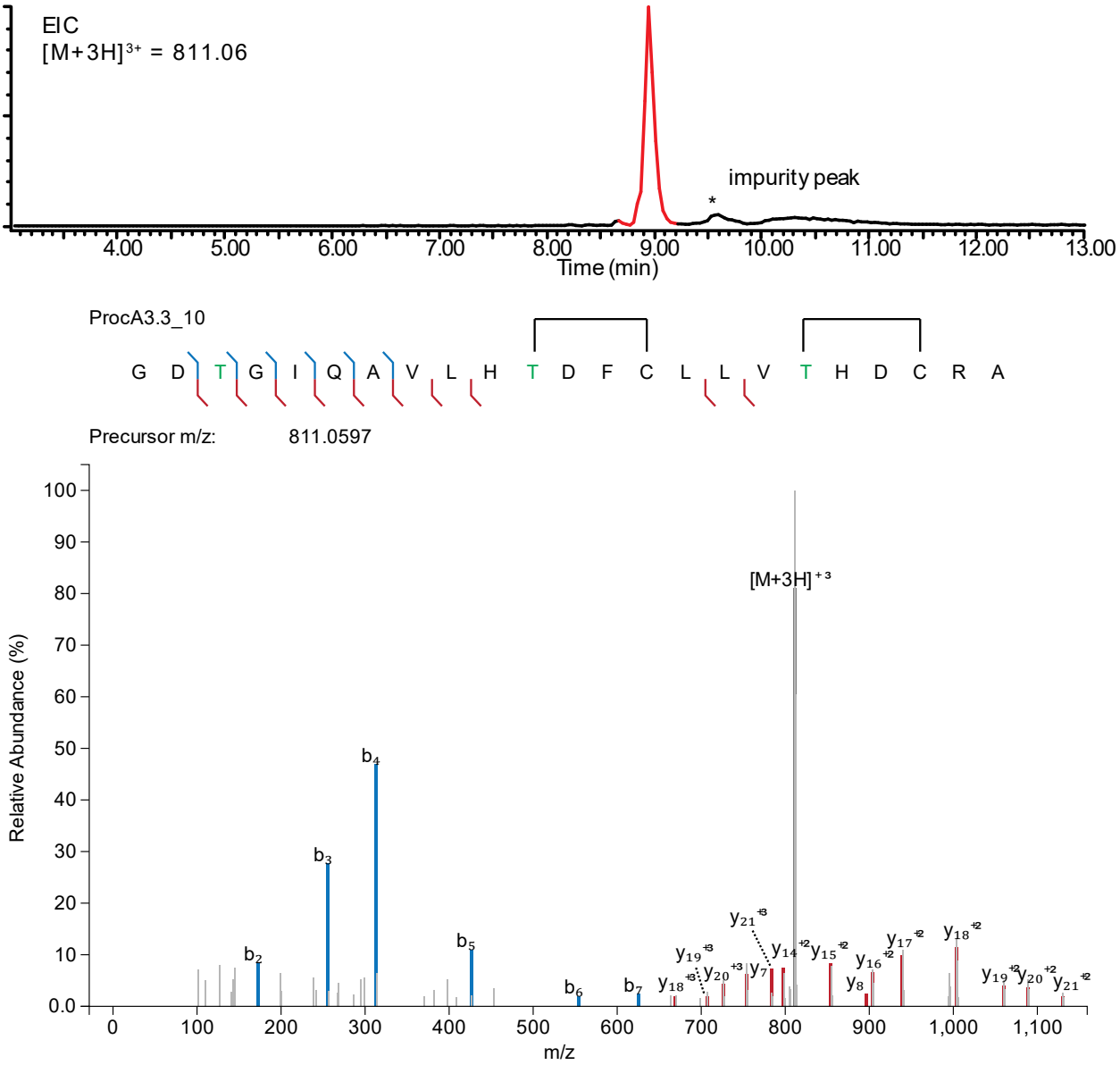

ion	charge	Observed mass	Theoretical mass	Error (ppm)
b2	1	173.0559	173.0557	1.2686
b3	1	256.0931	256.0928	1.1879
b4	1	313.1147	313.1143	1.4059
b5	1	426.1988	426.1983	1.1267
b6	1	554.2573	554.2569	0.7221
b7	1	625.2952	625.294	1.8971
y18	3	669.3304	669.3293	1.5734
y19	3	707.0255	707.024	2.0741
y20	3	726.0324	726.0312	1.669
y21	3	753.7115	753.7102	1.6894

y7	1	783.3571	783.3566	0.5943
y14	2	797.8674	797.8663	1.381
M+3H	3	811.0635	811.0597	4.6918
y15	2	854.4098	854.4083	1.7227
y8	1	896.4414	896.4407	0.787
y16	2	903.9441	903.9425	1.7312
y17	2	939.4625	939.4611	1.4986
y18	2	1003.492	1003.49	1.8116
y19	2	1060.034	1060.032	1.4979
y20	2	1088.545	1088.543	1.5212
y21	2	1130.064	1130.062	2.1222

Figure S11. LC-ESI-MS/MS analysis of ProcA3.3_11 modified by ProcM. (top) extracted ion chromatogram for the selected parent ion $[M+3H]^{3+}$; product with overlapping rings is shown in blue and product with non-overlapping rings is shown in red; (middle) MS/MS spectrum with b- (blue) and y- (red) ion fragments. (bottom) list of matched fragment ions showing theoretical masses, charge states, and mass error (ppm).

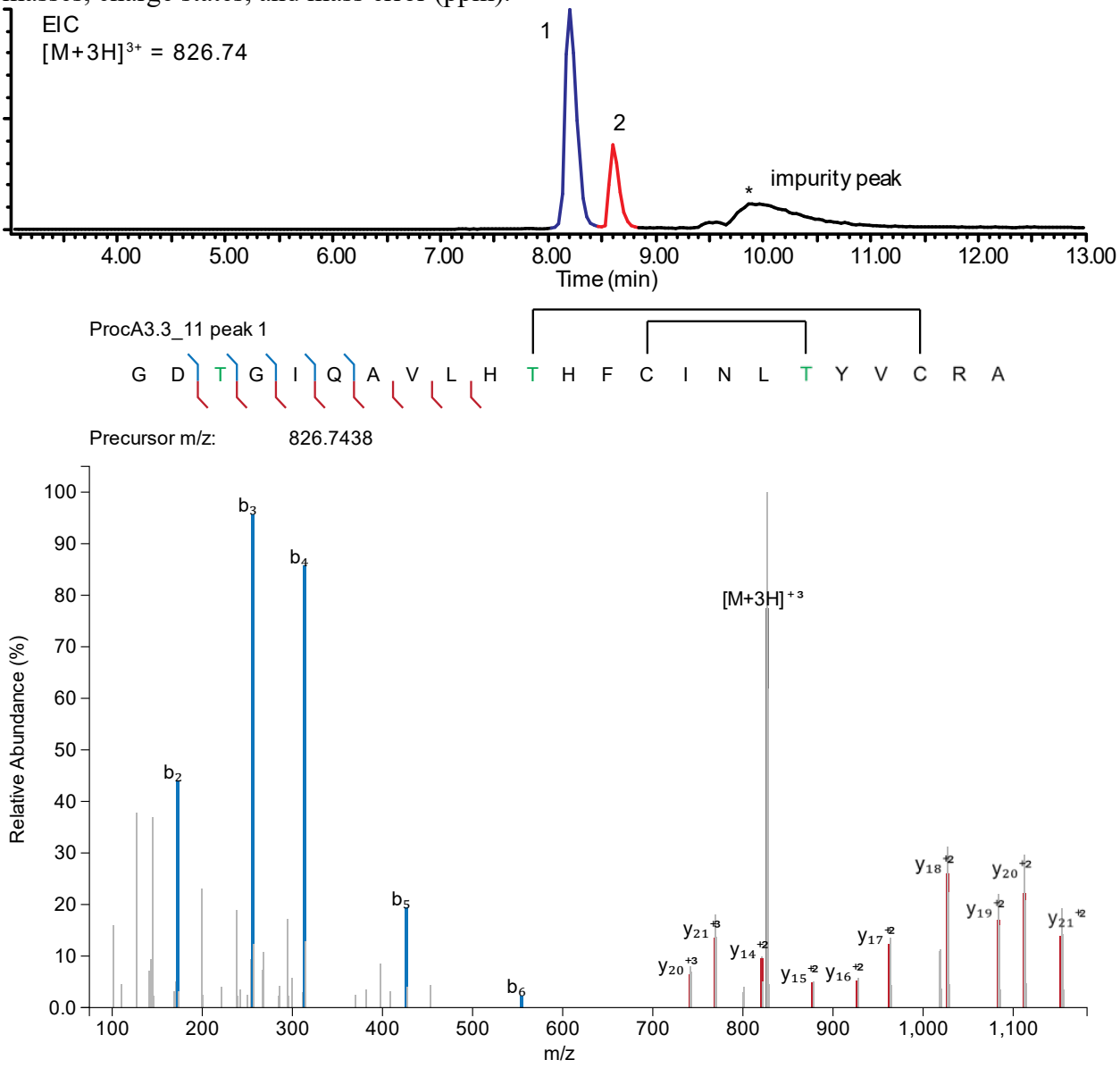

ion	charge	Observed mass	Theoretical mass	Error (ppm)
b2	1	173.0557	173.0557	0.1129
b3	1	256.093	256.0928	0.7974
b4	1	313.1145	313.1143	0.7672
b5	1	426.1983	426.1983	-0.0464
b6	1	554.2566	554.2569	-0.5409
y20	3	741.7154	741.7153	0.1147
y21	3	769.3947	769.3944	0.4506
y14	2	821.4045	821.3925	14.6238
M+3H	3	826.7459	826.7438	2.5143

y15	2	877.9345	877.9345	-0.0206
y16	2	927.4686	927.4687	-0.1349
y17	2	962.9875	962.9873	0.2262
y18	2	1027.017	1027.017	0.514
y19	2	1083.559	1083.559	0.6441
y20	2	1112.07	1112.069	0.6887
y21	2	1153.589	1153.588	0.7873

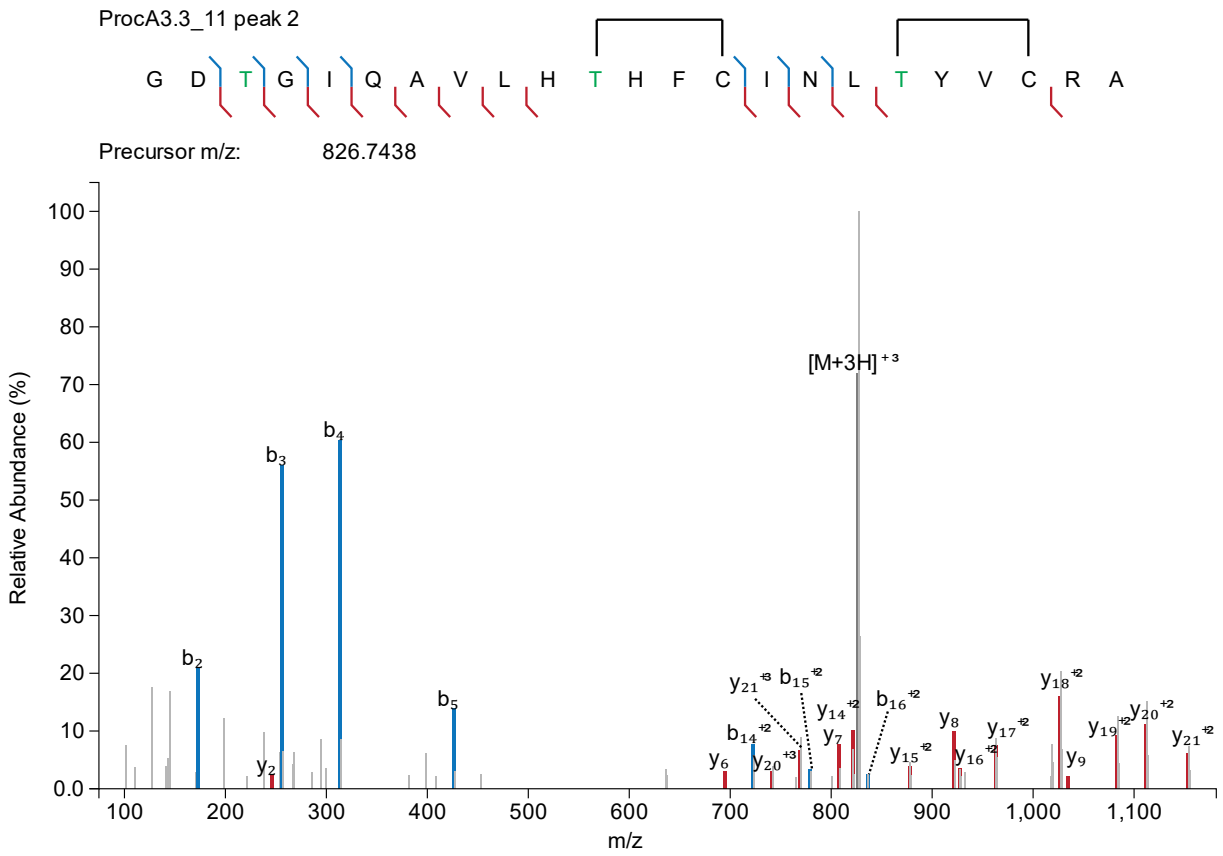

ion	charge	Observed mass	Theoretical mass	Error (ppm)
b2	1	173.0555	173.0557	-1.0428
y2	1	246.1556	246.1561	-1.8897
b3	1	256.0927	256.0928	-0.374
b4	1	313.1141	313.1143	-0.5103
b5	1	426.1982	426.1983	-0.281
y6	1	694.3341	694.3341	-0.0208
b14	2	722.8427	722.8431	-0.6222
y20	3	741.7152	741.7153	-0.1549
y21	3	769.3944	769.3944	0.0606
b15	2	779.385	779.3852	-0.2307
y7	1	807.418	807.4182	-0.2161
y14	2	821.4036	821.3925	13.5281
M+3H	3	826.7448	826.7438	1.1837
b16	2	836.406	836.4066	-0.7709

y15	2	877.9347	877.9345	0.2072
y8	1	921.4608	921.4611	-0.3304
y16	2	927.4689	927.4687	0.1886
y17	2	962.9876	962.9873	0.3301
y18	2	1027.016	1027.017	-0.3623
y9	1	1034.545	1034.545	-0.159
y19	2	1083.559	1083.559	0.2749
y20	2	1112.07	1112.069	0.5088
y21	2	1153.589	1153.588	0.6139

Figure S12. Chiral GC-MS analysis of ProcM-modified ProcA3.3 peptides. Chiral GC-MS analysis of ProcM-modified ProcA3.3_6 (A,B) and ProcA3.3_2 (C) core peptide fragments; panel A shows data from peak 1, panel B data for peak 2 of the LC of ProcA3.3_6. See Materials and Methods for derivatization of the amino acids. For each set of traces, derivatized samples are shown in blue (overlapping ring) and red (non-overlapping) and samples spiked with synthetic standards (DL- or LL-MeLan, as indicated) are shown below in orange and gray, respectively. Traces were selected-ion chromatograms monitoring for m/z = 379, which corresponds to the characteristic mass fragment for MeLan. Retention times drift slightly and therefore coinjections with authentic standards were used to verify assignments.

A

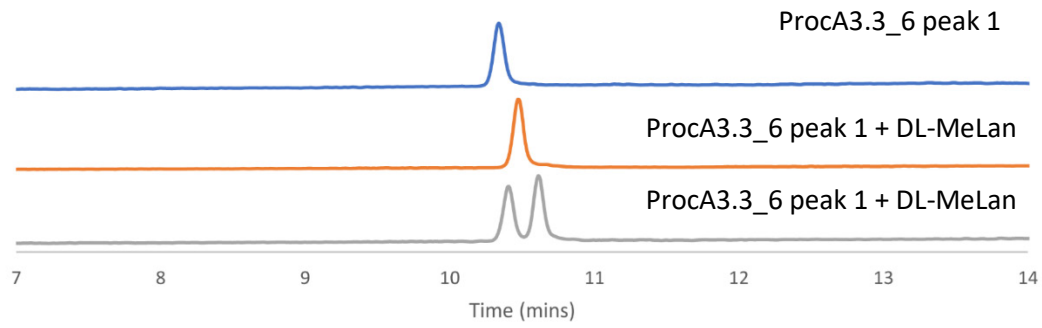

B

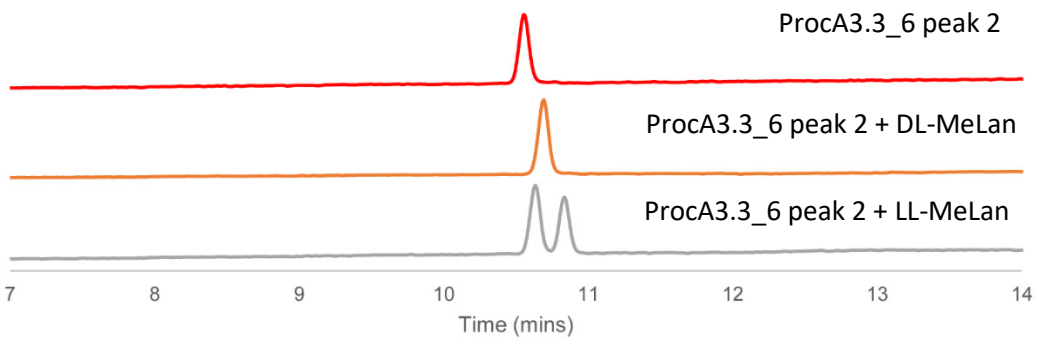

C

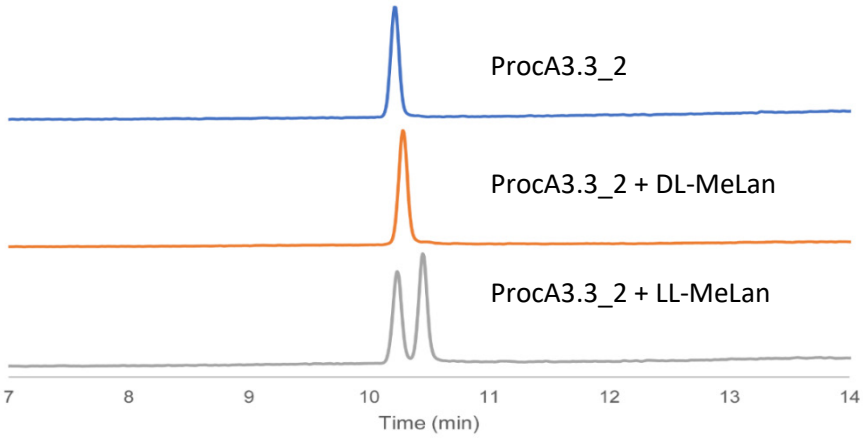

Figure S13. TIMS-MS/MS spectra of ProcM-modified ProcA3.3_4.

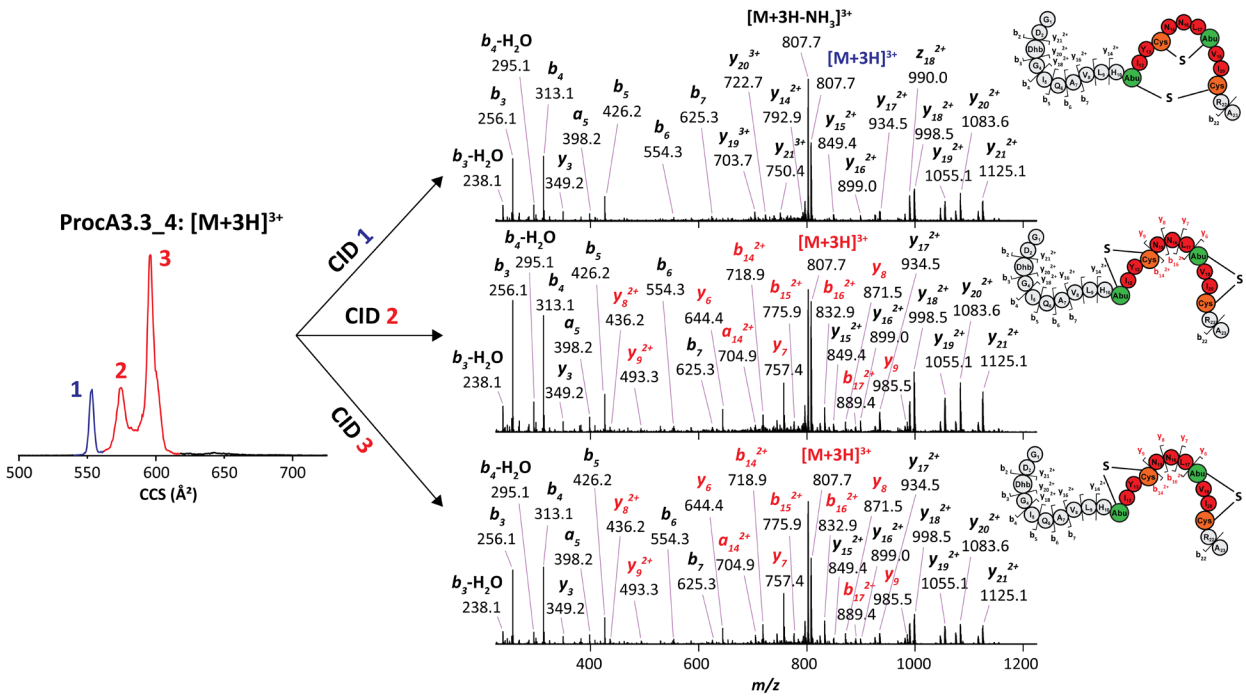

Figure S14. TIMS-MS/MS spectra of ProcM-modified ProcA3.3_6.

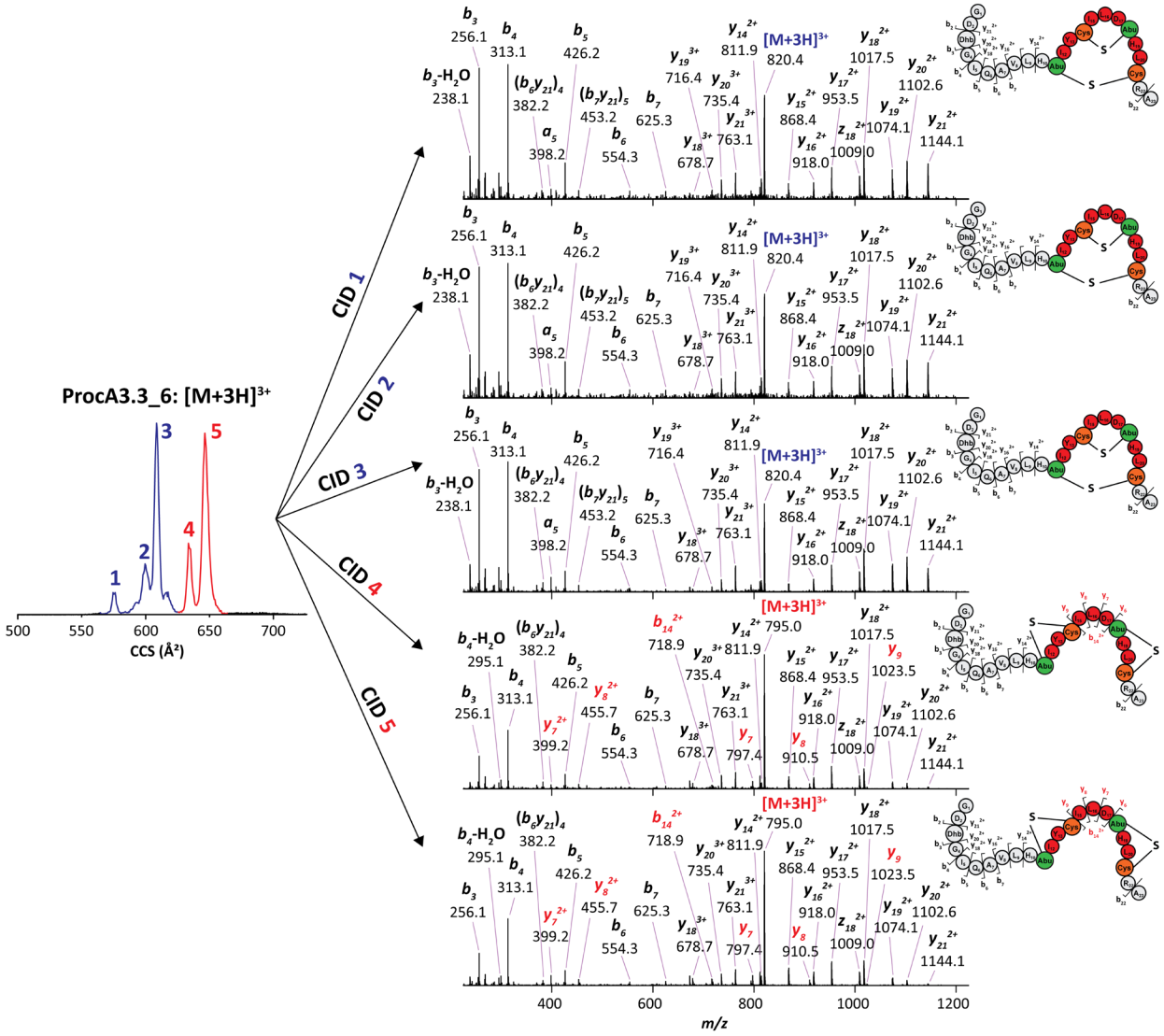

Figure S15. TIMS-MS/MS spectra of ProcM-modified ProcA3.3_1.

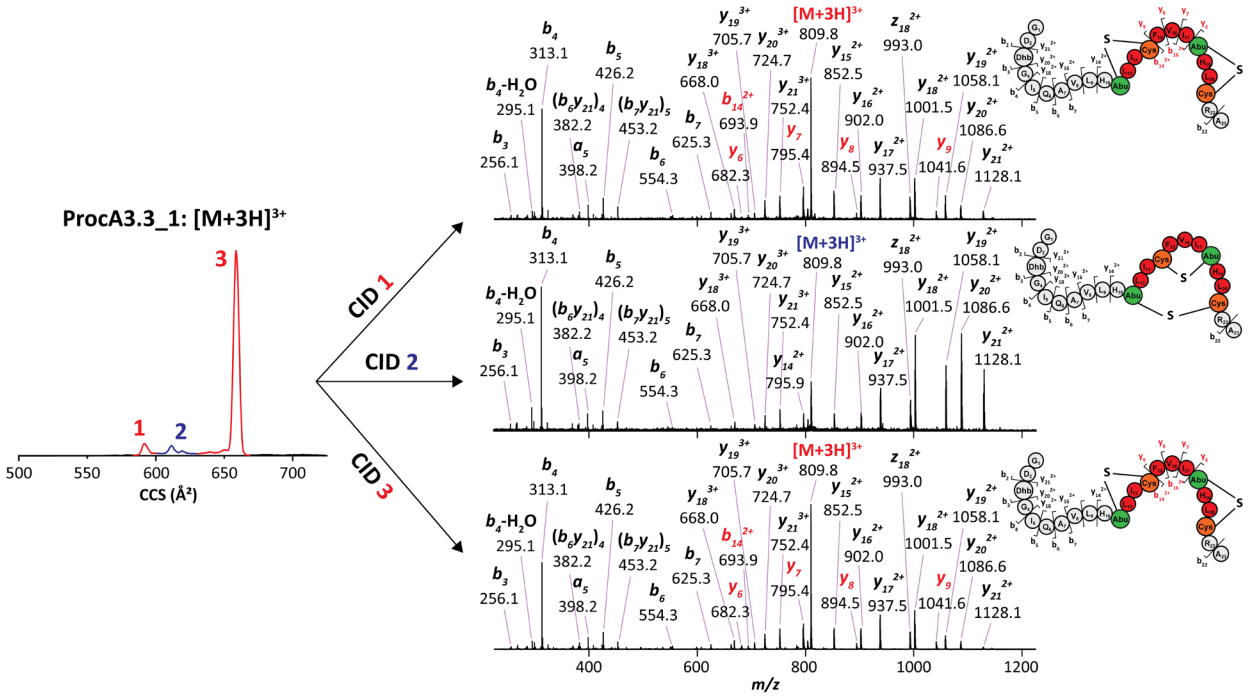

Figure S16. TIMS-MS/MS spectra of ProcM-modified ProcA3.3_9.

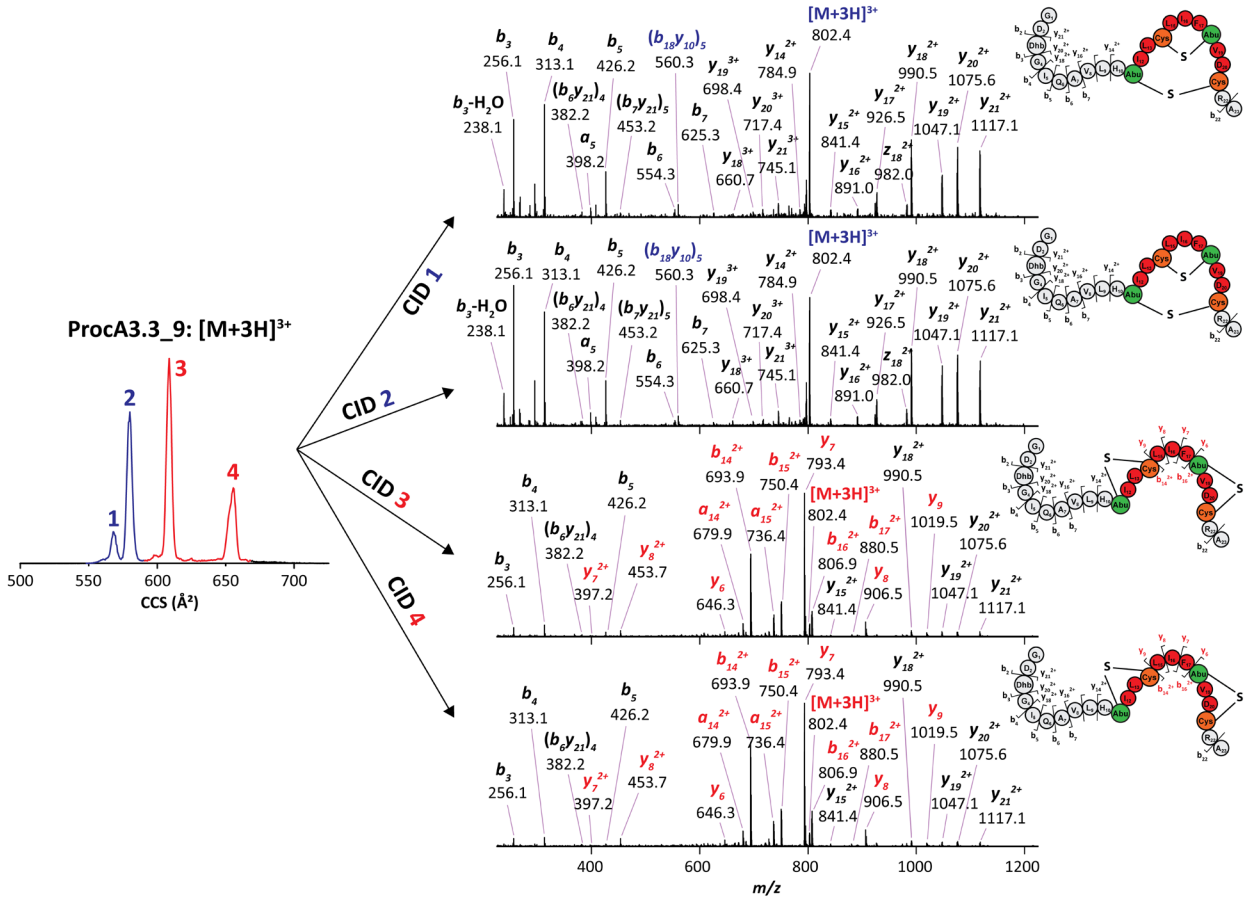

Figure S17. TIMS-MS/MS spectra of ProcM-modified ProcA3.3_10.

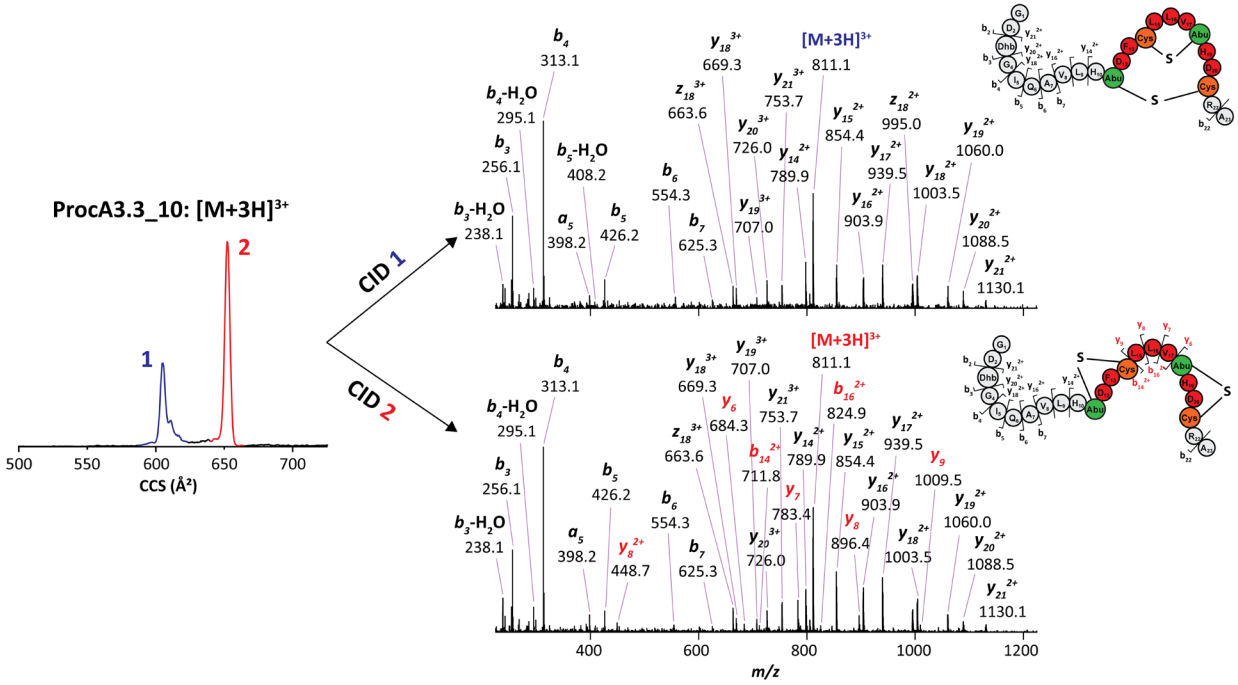

Figure S18. TIMS-MS/MS spectra of ProcM-modified ProcA3.3_5.

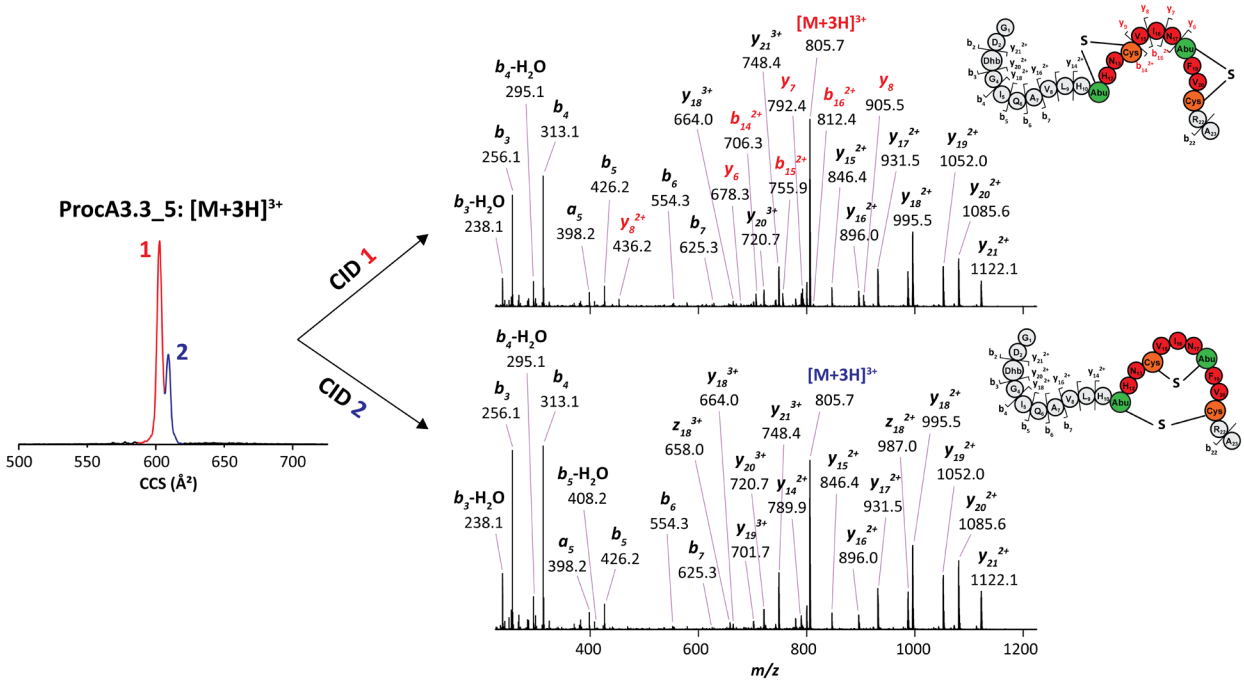

Figure S19. TIMS-MS/MS spectra of ProcM-modified ProcA3.3_11.

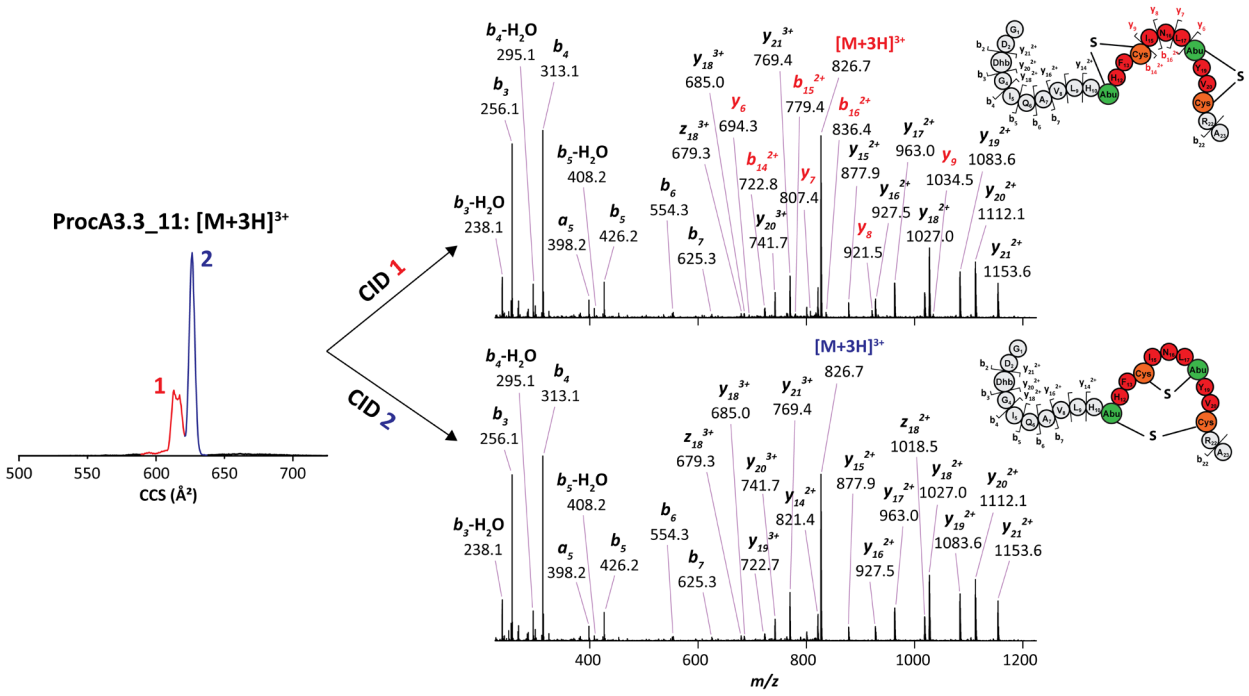

Figure S20. Structures of two additional prochlorosins containing two non-overlapping rings. Residues remaining from the leader peptide in prochlorosin 4.3 are indicated in italic font. See also Table 1.

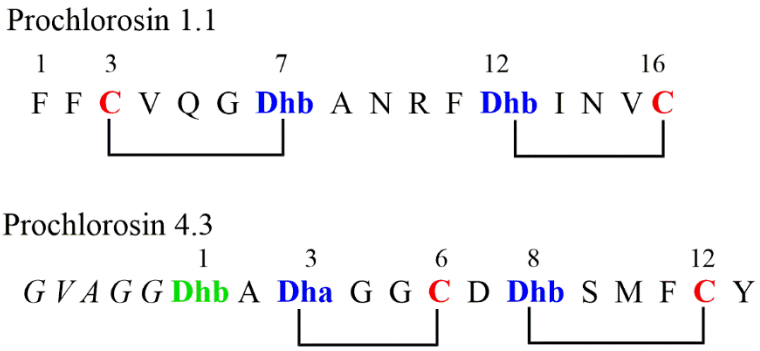

Figure S21. Relative energy (ΔE) of the different conformational configurations of each isomer of the analyzed prochlorosins after minimization, ordered from lower to higher energies.

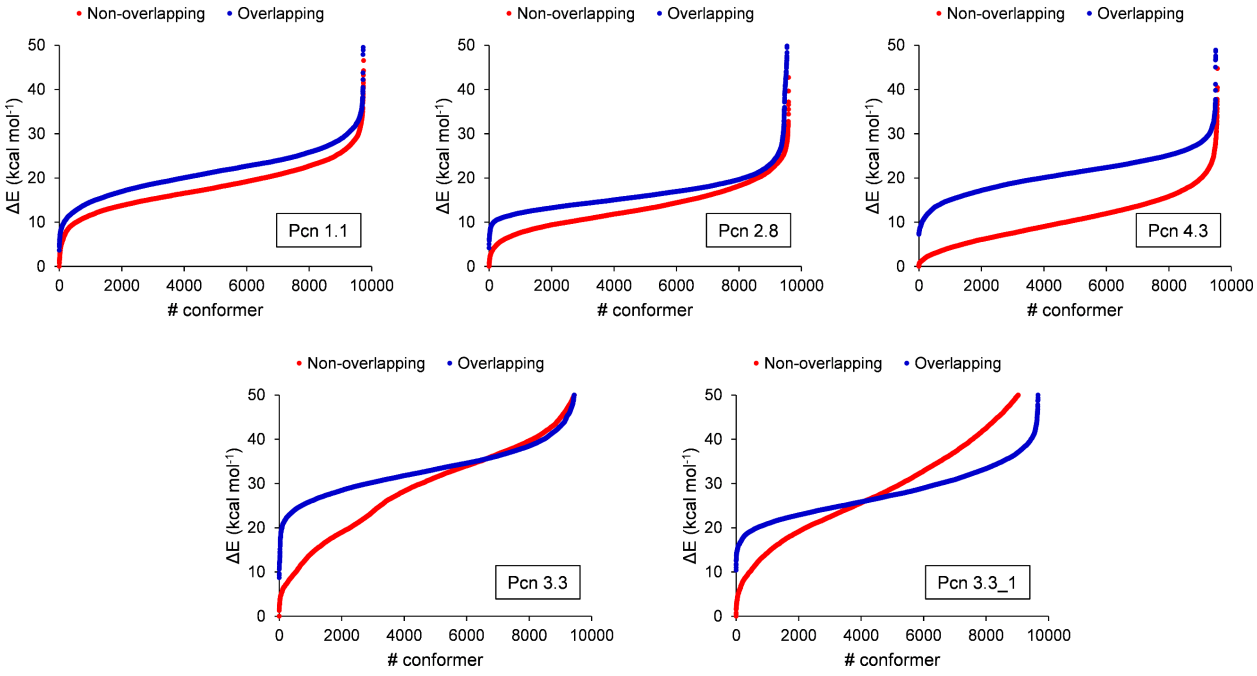

Figure S22. Backbone dihedral angles (φ/ψ) distribution derived from 1 μs MD simulations for amino acids Abu11 to L-Ala21 in Pcn 3.3 WT with overlapping ring pattern.

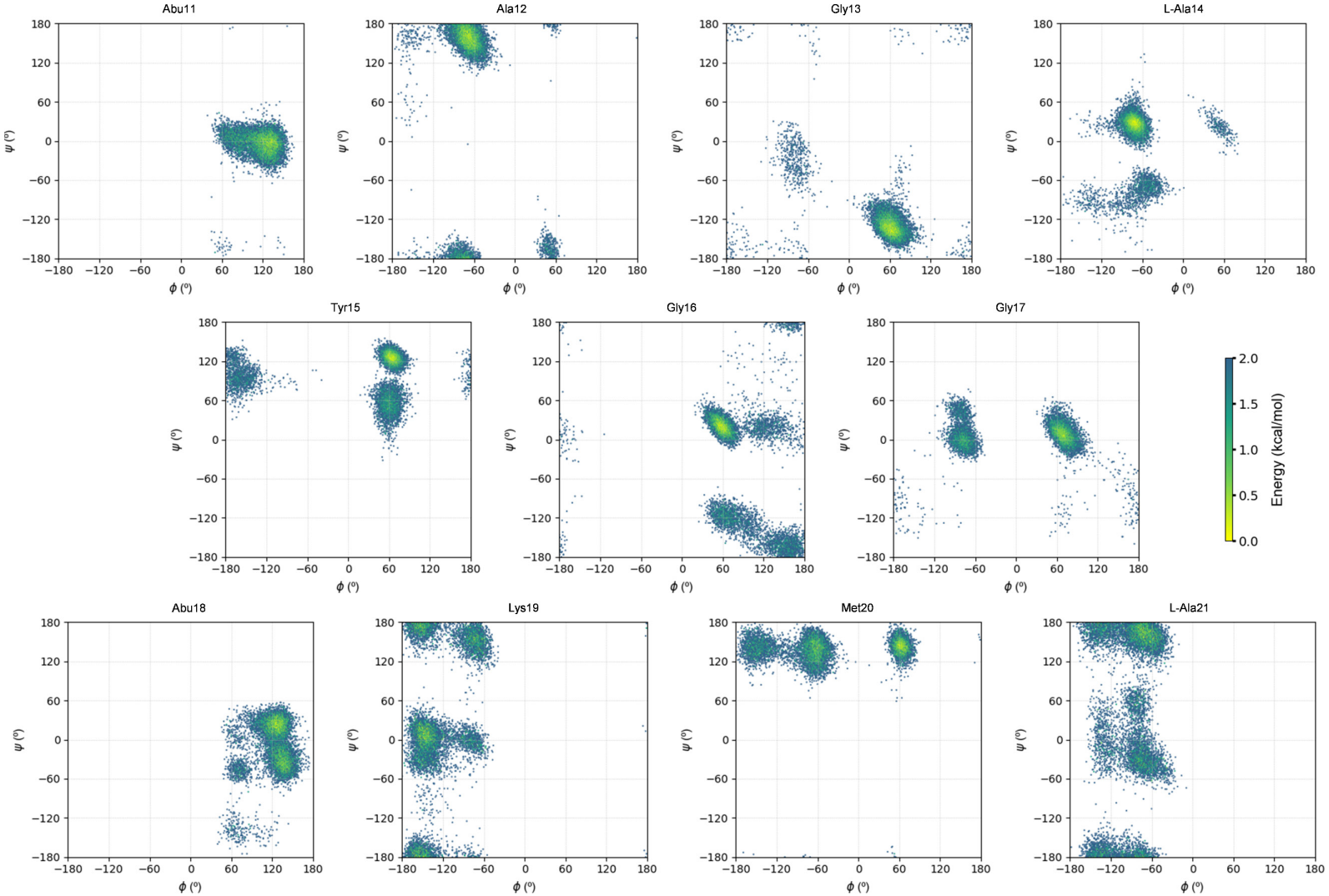

Figure S23. Backbone dihedral angles (φ/ψ) distribution derived from 1 μs MD simulations for amino acids Abu11 to L-Ala21 in Pcn 3.3 WT with non-overlapping ring pattern.

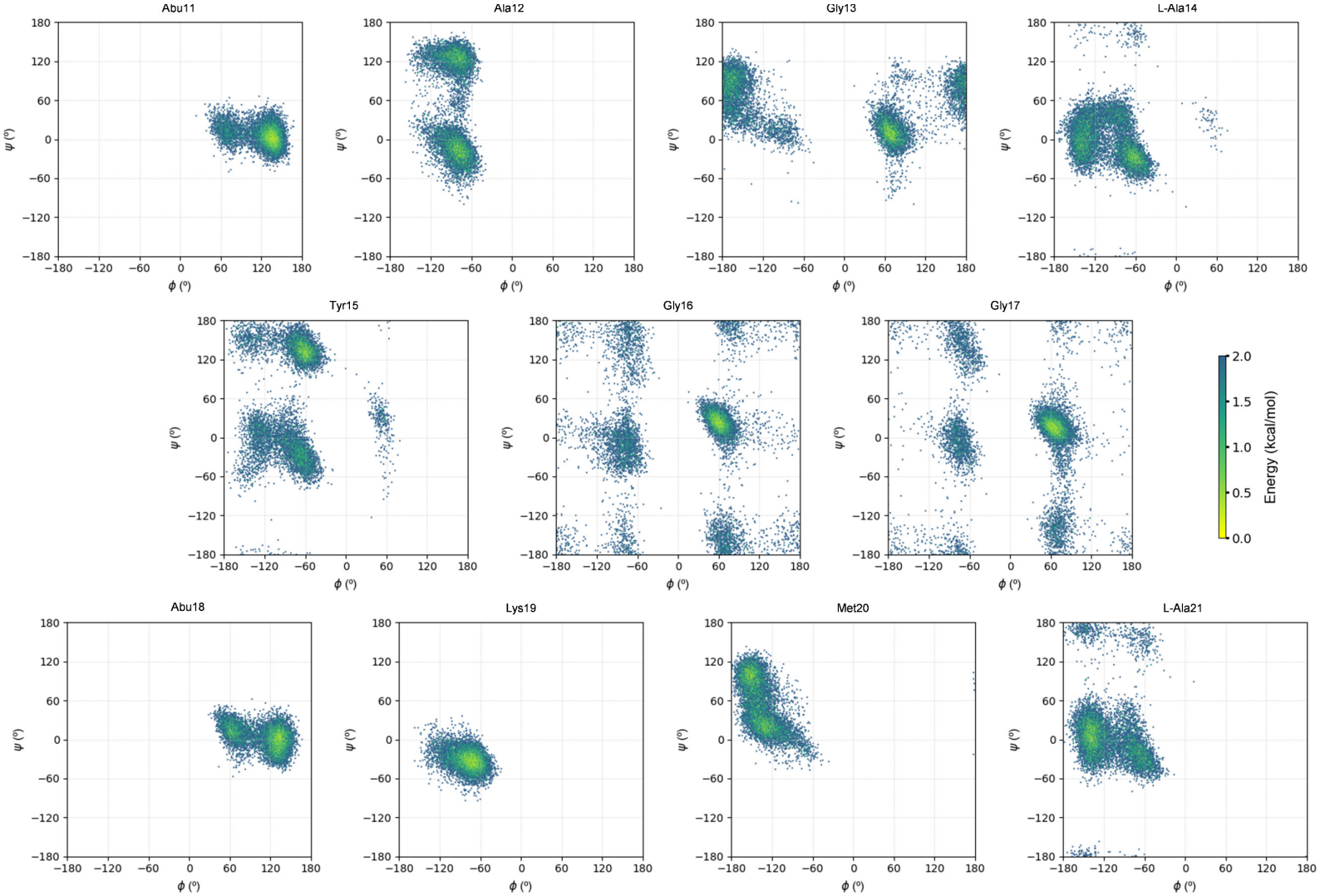

Figure S24. Backbone dihedral angles (φ/ψ) distribution derived from 1 μs MD simulations for amino acids Abu11 to L-Ala21 in Pcn 3.3_1 with overlapping ring pattern.

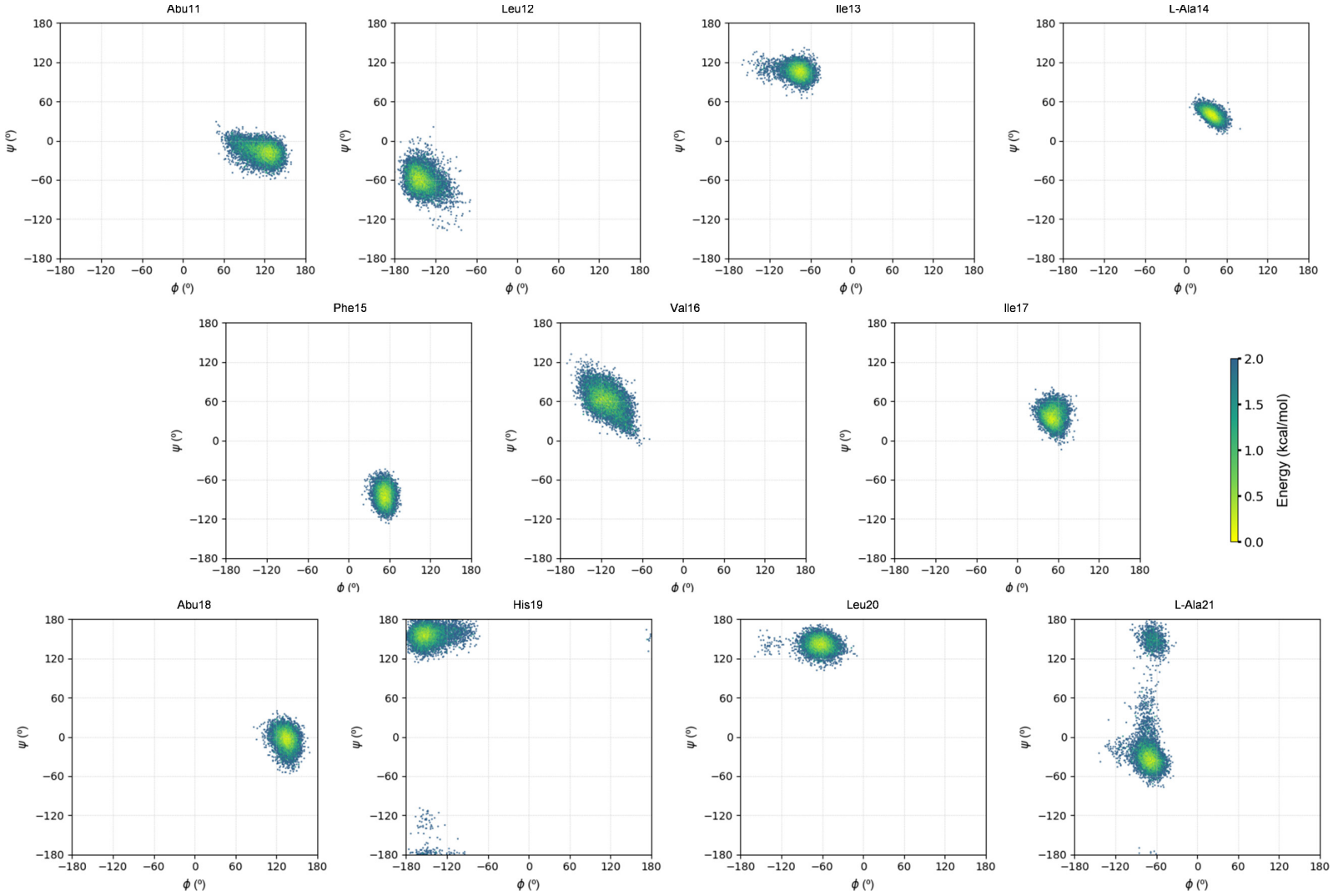

Figure S25. Backbone dihedral angles (φ/ψ) distribution derived from 1 μs MD simulations for amino acids Abu11 to L-Ala21 in Pcn 3.3_1 with non-overlapping ring pattern.

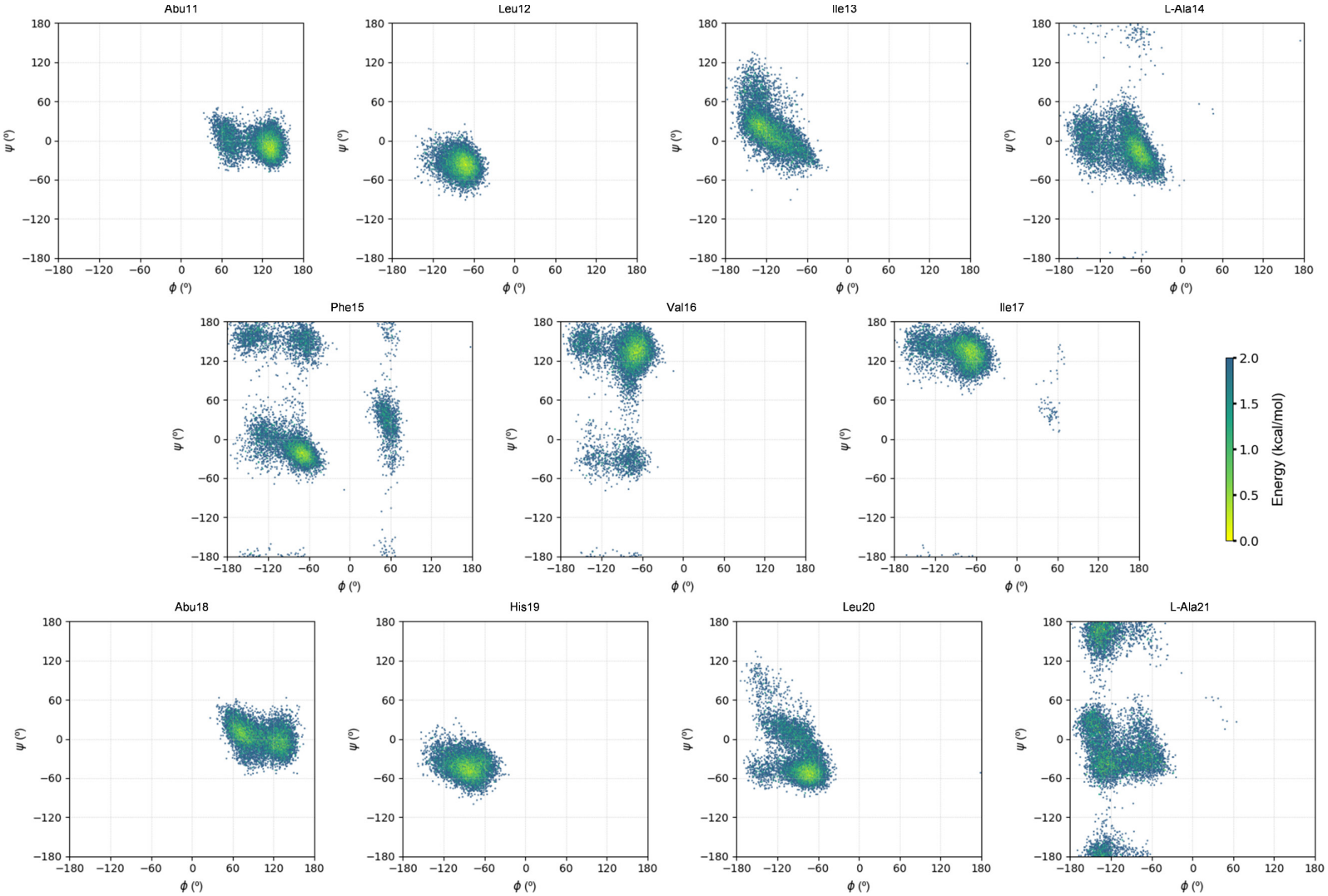

Figure S26. TIMS-MS/MS analysis of ProcA WT-Y15F/G16V/G17I.

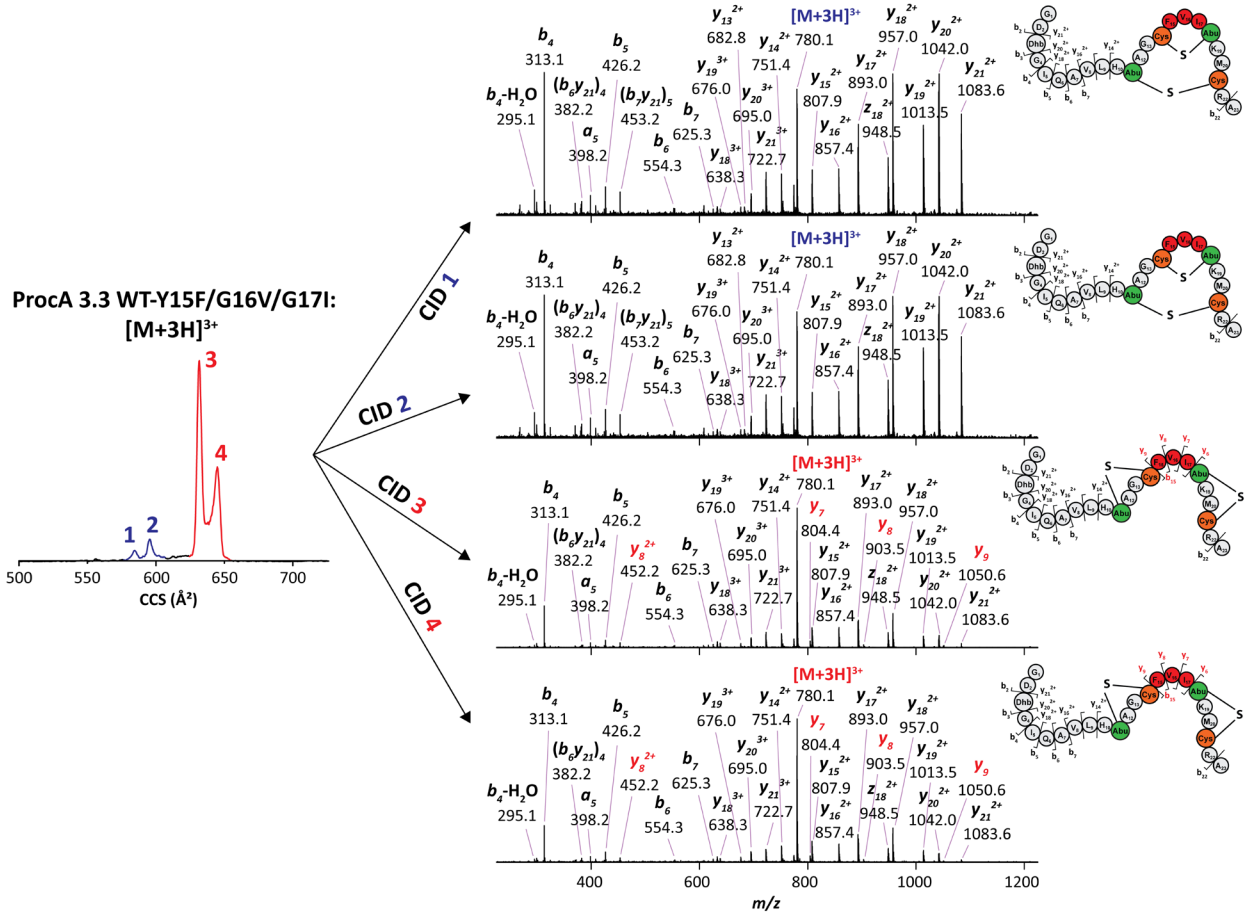

Figure S27. TIMS-MS/MS analysis of ProcA3.3_10-L15Y/L16G/V17G).

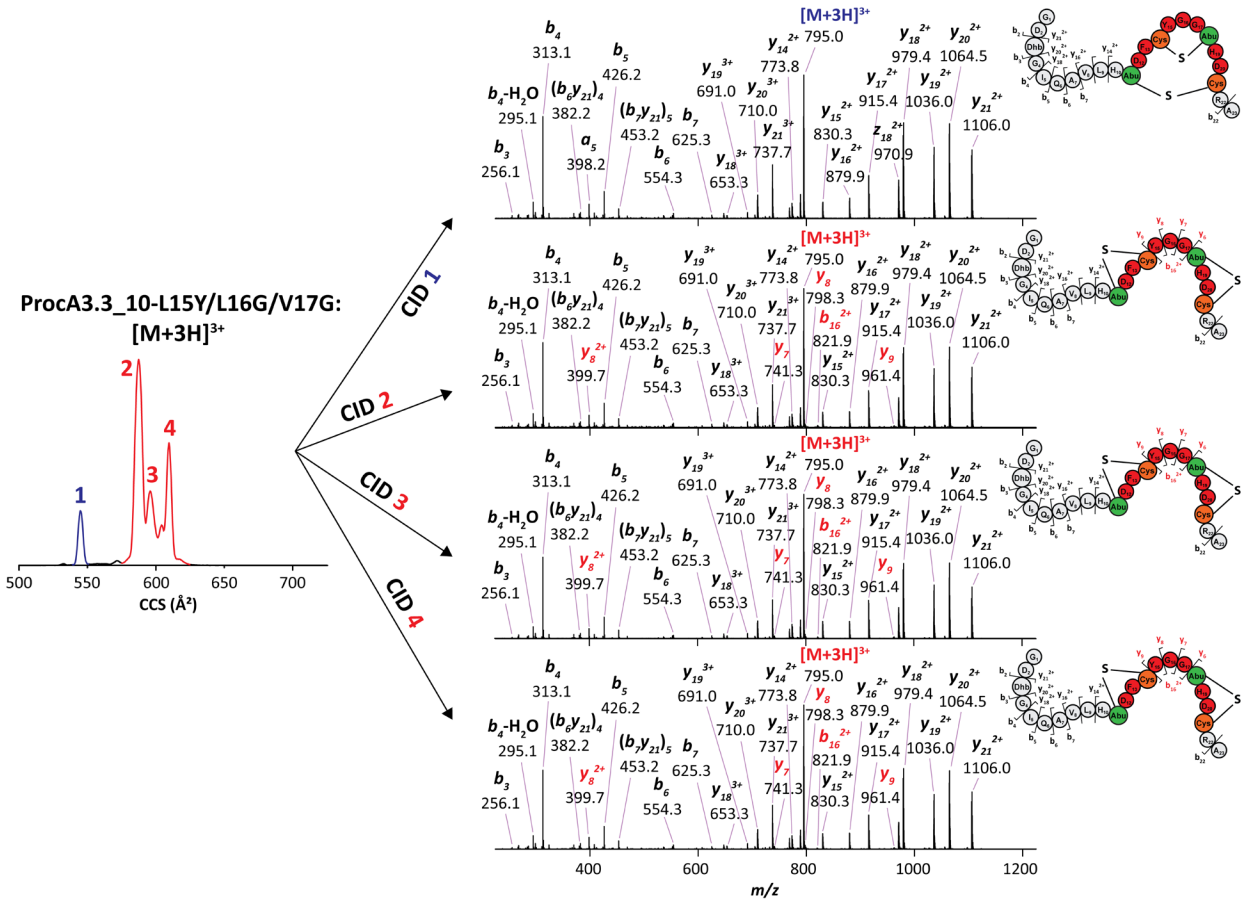

Figure S28. LC-ESI-MS/MS analysis of ProcA3.3 WT-Y15L/G16L/G17V modified by ProcM. (A) (top) extracted ion chromatogram for the selected parent ion $[M+3H]^{3+}$; product with overlapping rings is shown in blue and product with non-overlapping rings is shown in red; (middle) MS/MS spectrum with b- (blue) and y- (red) ion fragments; (bottom) list of matched fragment ions showing theoretical masses, charge states, and mass error (ppm). (B) TIMS-MS/MS spectra of ProcA3.3 WT-Y15L/G16L/G17V.

A

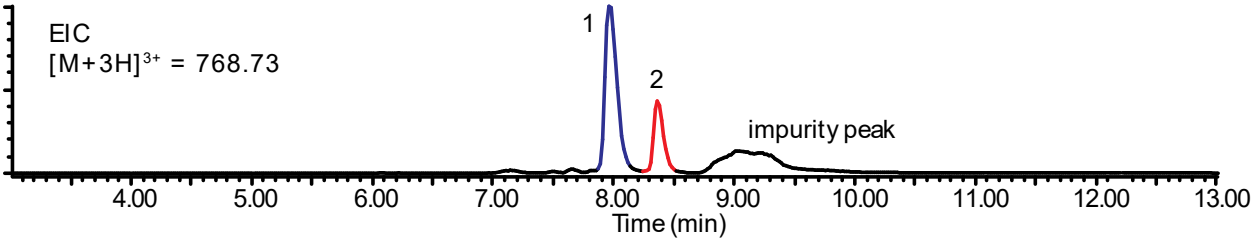

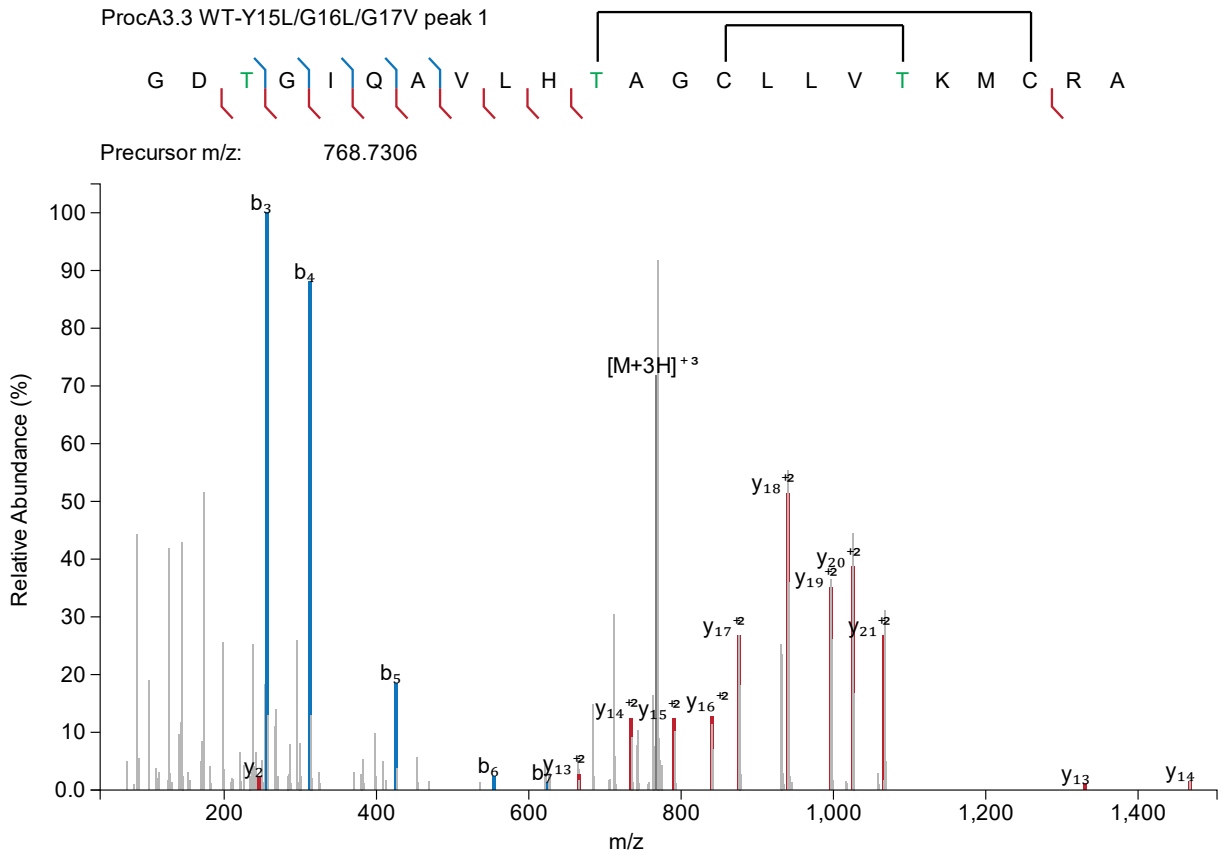

ion	charge	Observed mass	Theoretical mass	Error (ppm)
y2	1	246.1576	246.1561	6.1158
b3	1	256.0857	256.0928	-27.6626
b4	1	313.1108	313.1143	-11.1872

b5	1	426.2012	426.1983	6.8309
b6	1	554.2709	554.2569	25.3415
b7	1	625.2985	625.294	7.1602
y13	2	665.8409	665.8433	-3.4909
y14	2	734.3664	734.3727	-8.5902
M+3H	3	768.7146	768.7306	-20.9135
y15	2	790.9175	790.9147	3.5149
y16	2	840.4463	840.4489	-3.1213
y16	2	840.4689	840.4489	23.7424
y17	2	875.974	875.9675	7.4025
y18	2	939.9915	939.9968	-5.6761
y19	2	996.538	996.5388	-0.8064
y20	2	1025.034	1025.05	-14.8306
y21	2	1066.569	1066.568	0.4718
y13	1	1330.658	1330.679	-16.0661
y13	1	1330.7	1330.679	15.7748
y14	1	1467.709	1467.738	-19.6832
y14	1	1467.74	1467.738	1.018
y14	1	1467.77	1467.738	21.7343

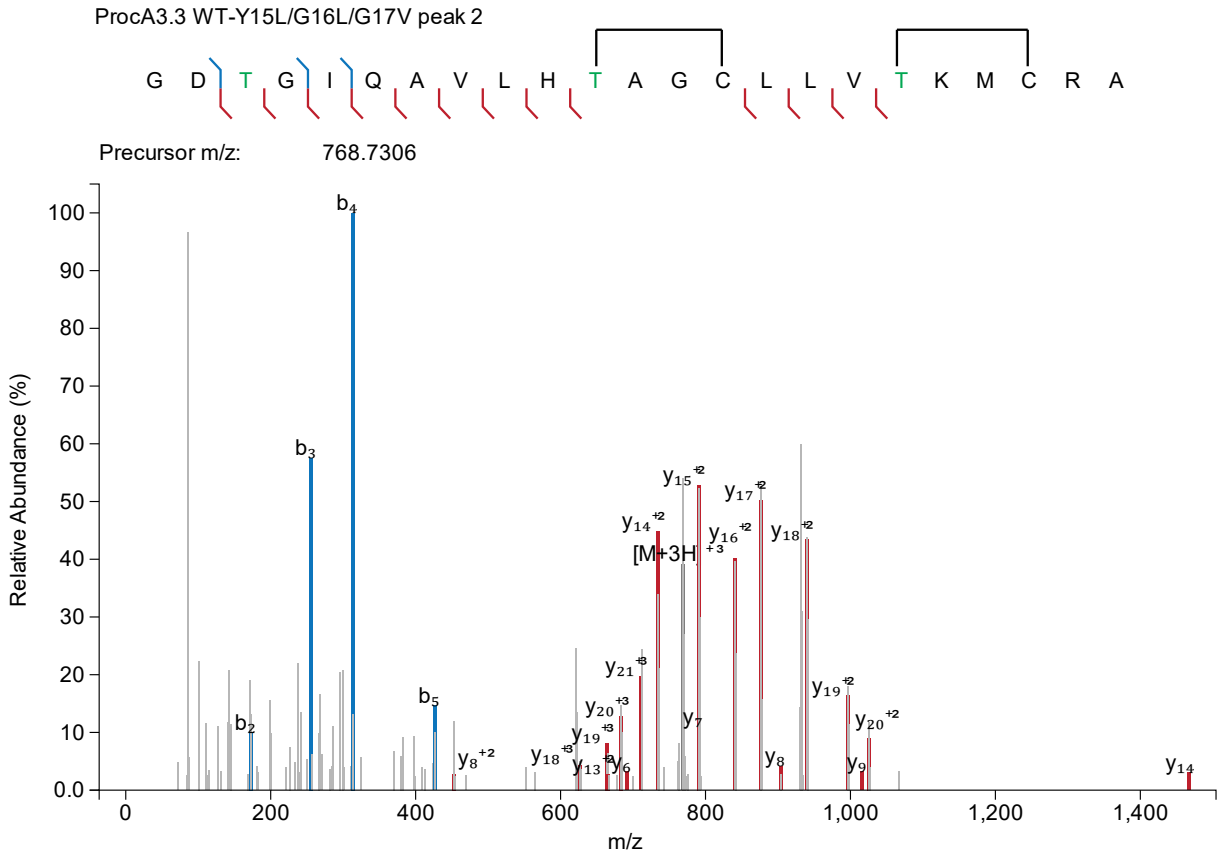

ion	charge	Observed mass	Theoretical mass	Error (ppm)
b2	1	173.0523	173.0557	-19.7466
b3	1	256.0982	256.0928	20.9823
b4	1	313.1183	313.1143	13.0624
b5	1	426.1988	426.1983	1.1422
y8	2	452.2553	452.2488	14.4479
y18	3	626.9902	627.0003	-16.0627
y18	3	627.0095	627.0003	14.772
y19	3	664.686	664.695	-13.551
y13	2	665.8336	665.8433	-14.4625
y20	3	683.7047	683.7021	3.7126
y6	1	691.332	691.3378	-8.3435
y21	3	711.3866	711.3812	7.6038
y14	2	734.3725	734.3727	-0.2656
M+3H	3	768.7337	768.7306	3.9663
y7	1	790.4054	790.4062	-1.0587
y15	2	790.9188	790.9147	5.0805
y16	2	840.4396	840.4489	-11.1011
y17	2	875.9493	875.9675	-20.7451
y17	2	875.9807	875.9675	15.0157
y8	1	903.5021	903.4903	13.1206
y18	2	939.9939	939.9968	-3.0443
y19	2	996.5222	996.5388	-16.7263
y9	1	1016.575	1016.574	0.9911
y20	2	1025.038	1025.05	-11.0991
y20	2	1025.076	1025.05	25.7362
y14	1	1467.715	1467.738	-15.705
y14	1	1467.761	1467.738	15.2345

B

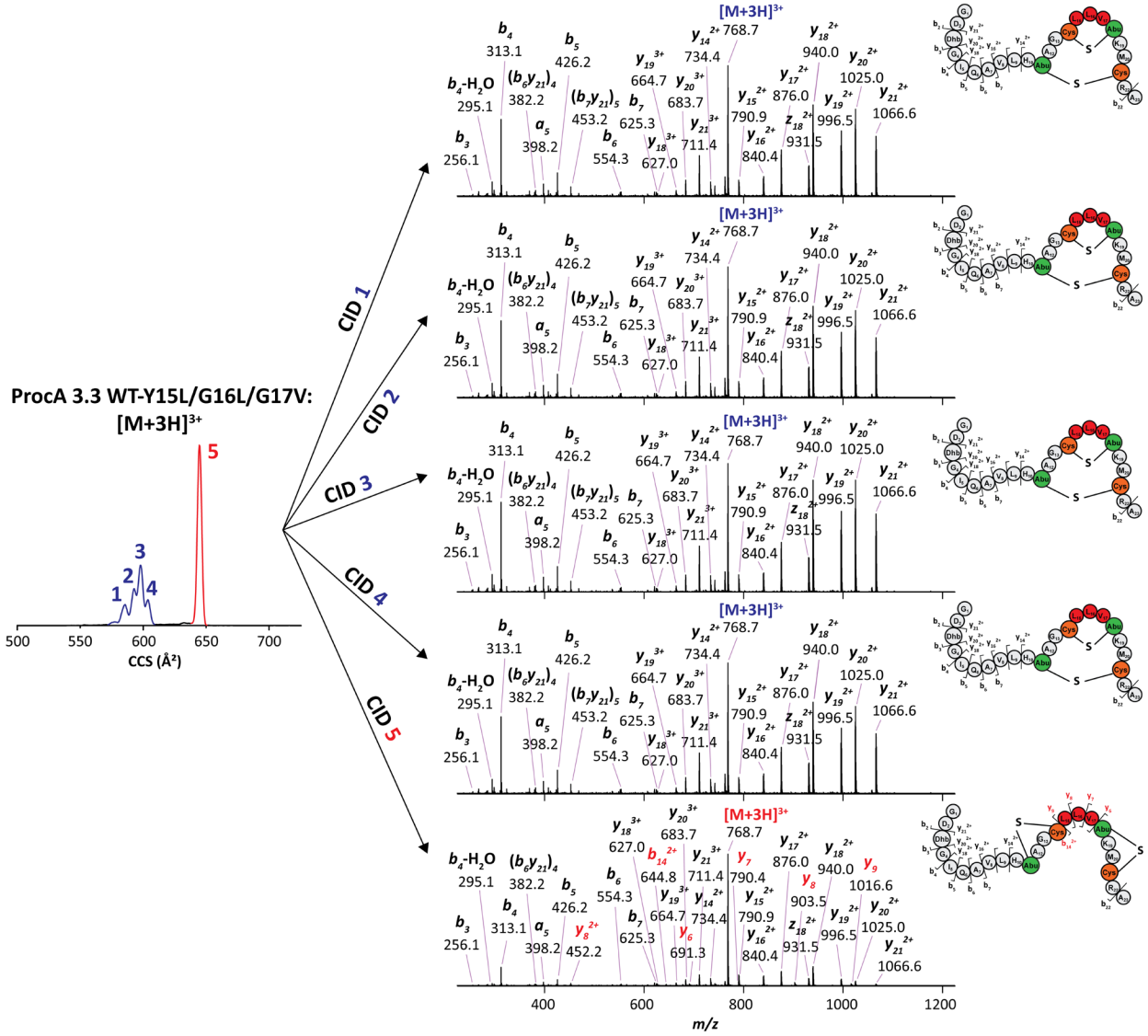
ProcA 3.3 WT-Y15L/G16L/G17V:
[M+3H]3+
5
3
2
1
4
500
550
600
650
700
CCS (Å²)
CID 1
CID 2
CID 3
CID 4
CID 5
[M+3H]3+
400
600
800
1000
1200
m/z

Figure S29. Comparison of the data of the extracted TIMS spectra from the mixture of peptide with data from individual purified peptides (insets). As reported previously, ProcM-C971H in which one of the Cys ligands to the Zn^{2+} in the active site of the cyclization domain is mutated to His also produces a mixture of products, which was used as a control.[21]

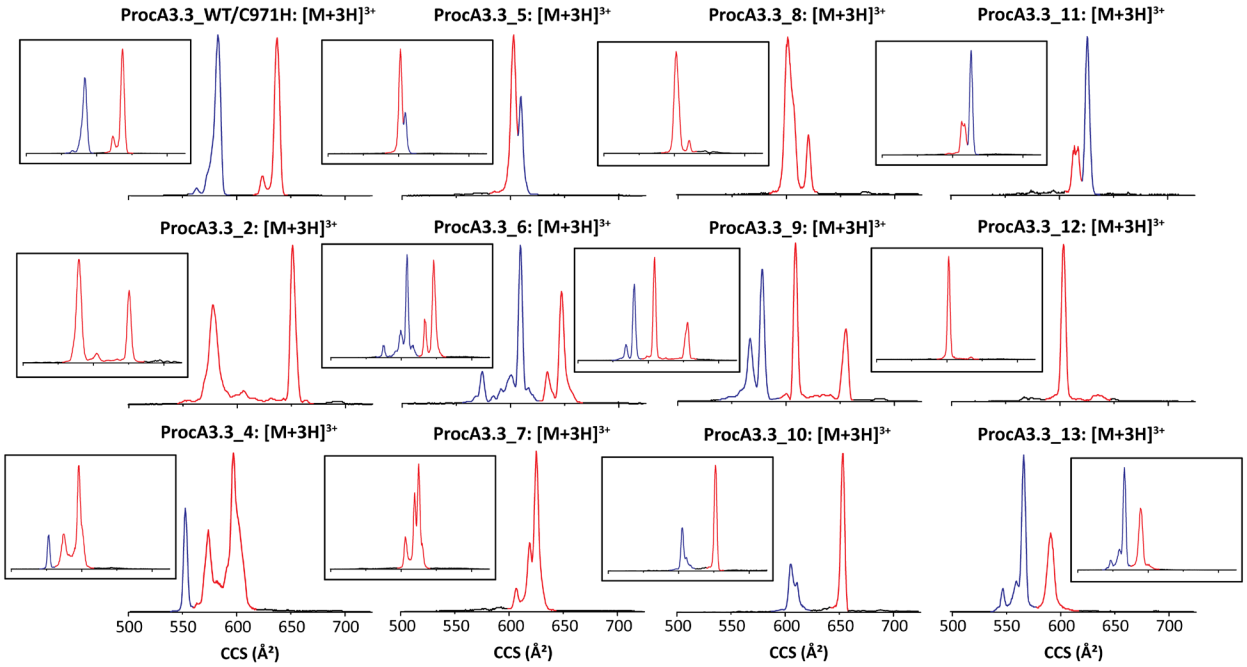

Figure S30. LC-ESI-MS/MS analysis of ProcA3.3_13 modified by ProcM. (top) extracted ion chromatogram for the selected parent ion $[M+3H]^{3+}$; product with overlapping rings is shown in blue and product with non-overlapping rings is shown in red; (middle) MS/MS spectrum with b- (blue) and y- (red) ion fragments (bottom) list of matched fragment ions showing theoretical masses, charge states, and mass error (ppm).

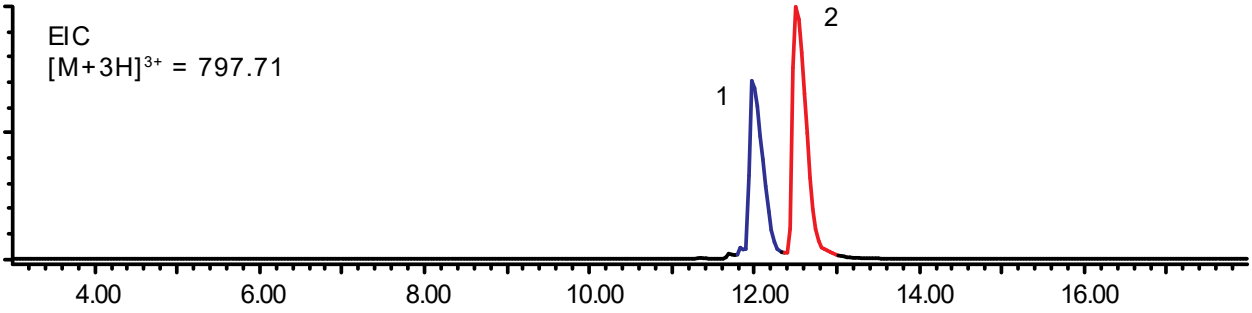

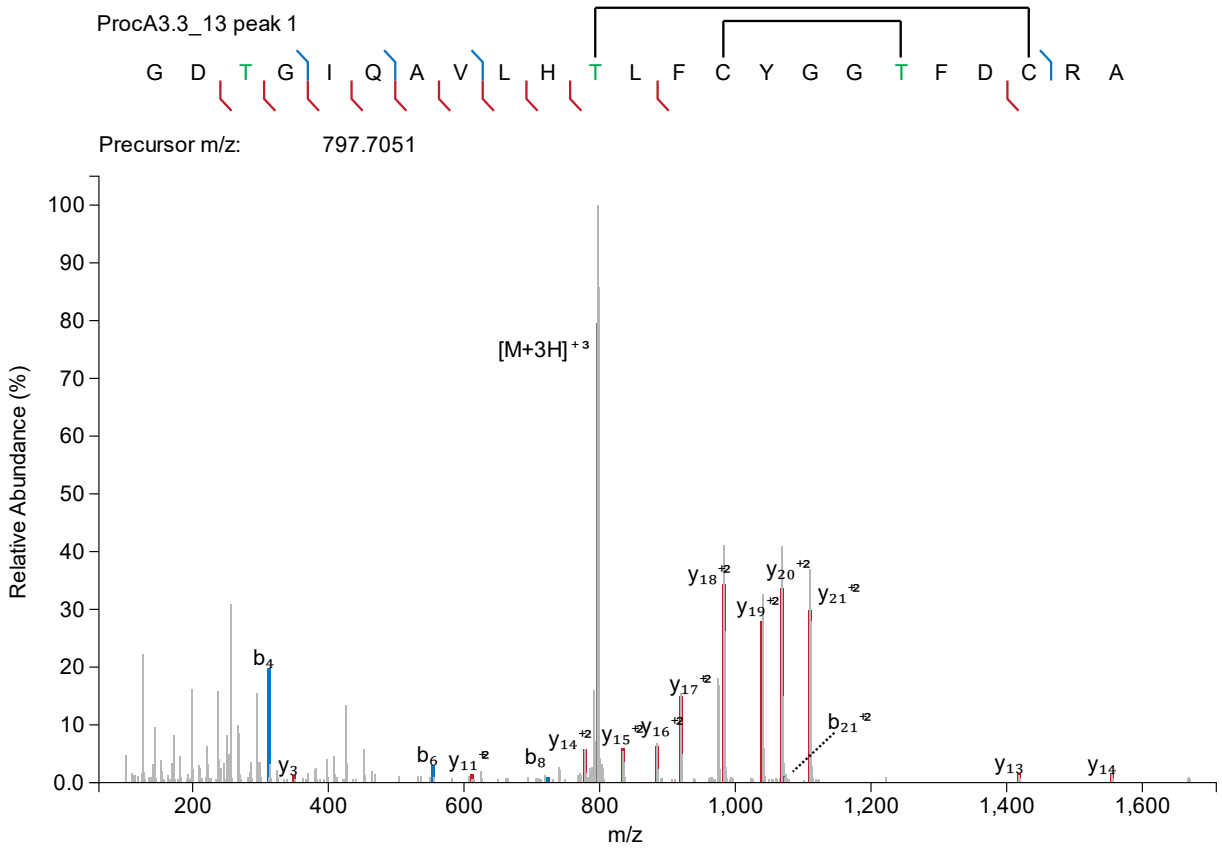

ion	charge	Observed mass	Theoretical mass	Error (ppm)
b4	1	313.1151	313.1143	2.7185
y3	1	349.1679	349.1653	7.567
b6	1	554.2659	554.2569	16.2727
y11	2	611.2496	611.2444	8.402
b8	1	724.3691	724.3624	9.2168
y14	2	777.8412	777.8345	8.6728
M+3H	3	797.6984	797.7051	-8.4459
y15	2	834.3706	834.3765	-7.077
y16	2	883.9076	883.9107	-3.5152
y17	2	919.4296	919.4293	0.3439
y18	2	983.466	983.4586	7.5379
y19	2	1040.0104	1040.0006	9.4235
y20	2	1068.5098	1068.5113	-1.4328
b21	2	1073.4741	1073.4797	-5.246
y21	2	1110.0403	1110.0299	9.381
y13	1	1417.6289	1417.6028	18.4388
y14	1	1554.6753	1554.6617	8.7838

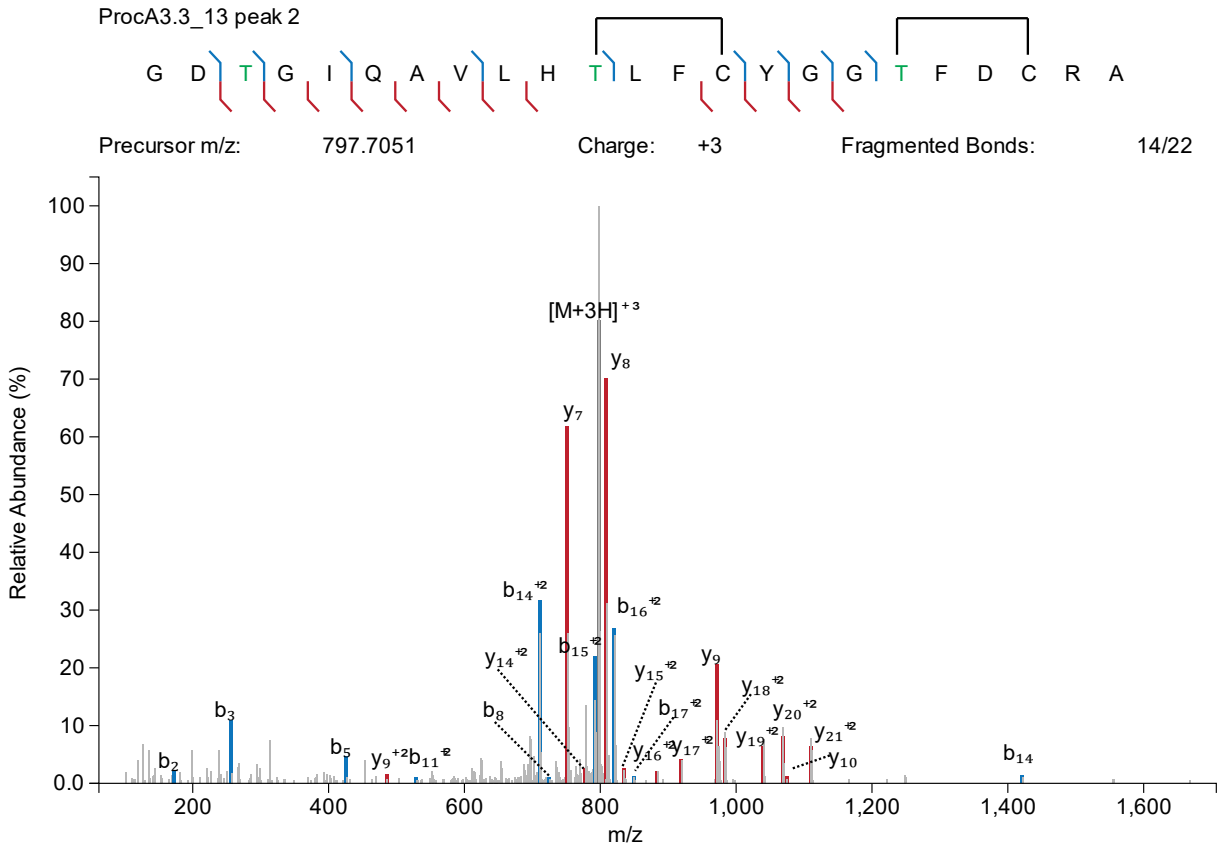

ion	charge	Observed mass	Theoretical mass	Error (ppm)
b2	1	173.0541	173.0557	-9.3989
b3	1	256.0909	256.0928	-7.541
b5	1	426.1984	426.1983	0.1162
y9	2	486.2092	486.2056	7.3939
b11	2	529.2837	529.2749	16.6009
b14	2	710.8579	710.8557	3.1201
b8	1	724.3734	724.3624	15.1564
y7	1	751.3286	751.3192	12.5643
y14	2	777.8298	777.8345	-5.9682
b15	2	792.3746	792.3874	-16.1666
M+3H	3	797.702	797.7051	-3.9426
y8	1	808.3418	808.3406	1.4644
b16	2	820.9038	820.8981	6.8811
y15	2	834.3739	834.3765	-3.106
b17	2	849.4179	849.4089	10.7058
y16	2	883.9103	883.9107	-0.4362
y17	2	919.4319	919.4293	2.8415
y9	1	971.4049	971.404	0.9673
y18	2	983.4523	983.4586	-6.3379
y19	2	1039.9962	1040.0006	-4.2139
y20	2	1068.5102	1068.5113	-1.0717
y10	1	1074.4128	1074.4132	-0.3775

y21	2	1110.025	1110.0299	-4.3895
b14	1	1420.7114	1420.7042	5.1138

Table S3. Ring sizes of lanthionines/methyllanthionines in currently structurally characterized class II lanthipeptides. Only structurally unique compounds were analyzed;[22] structural homologs of the compounds in the table that are variants with the same ring patterns were not counted. The Lan or MeLan bisamino acids were counted as 2 amino acids (aa).

Compound	4-aa	5-aa	6-aa	Other (size)
Actagardine[23]			3	1 (9)
BhtA1[24]			1	2 (8,11)
BhtA2[24]	2	1		
Bicereucin B			1	
Birimositide B[22]	2	2		
Bovicin HJ50[25]			1	1 (23)
Carnolysin A1[26]		3		
Cerecidin A1-A7[27]		2		
Cinnamycin B[28]				3 (7,11,18)
$CylL_L$[29]		3		
$CylL_S$[29]		2		
Flavecin A1[26]	1		1	2 (8,11)
Geobacillin II[26]		3	1	
Haloduracin α[24]			1	2 (8,11)
Haloduracin β[24]	2	2		
Lacticin 481[28]			1	2 (9,15)
Lacticin 3147 α[25]			1	3 (2,8,11)
Lacticin 3147 β[25]	2	1		
Lichenidicidin α[30]		1	1	2 (8,11)
Lichenidicidin β[30]	2	2		
Mersacidin[28]			1	2 (2, 9)
Michiganin A[28]			2	1 (9)
Nukacin ISK-1[25]			1	2 (9,15)
Plantaricin C[31]	2		1	1 (21)
Prochlorosin 1.1[25]		2		
Prochlorosin 1.7[25]	1	1		1 (10)
Prochlorosin 2.1[32]	1		1	2 (9,9)
Prochlorosin 2.8[25]				2 (7,7)
Prochlorosin 2.11[25]		1		2 (7,7)
Prochlorosin 3.3[25]		1		1 (11)
Prochlorosin 4.3[25]	1	1		
Salivaricin A[33]			2	1 (11)
Salivaricin B[34]			1	2 (9,15)
Salivaricin E[34]			2	1 (11)
Total	16 (16%)	28 (27%)	23 (22%)	36* (35%)

* 7-aa rings: 5 (5%); 8-aa rings: 5 (5%); 9-aa rings: 8 (8%); 11-aa rings 9 (9%).

References Supporting Information

(1) Li, B.; Sher, D.; Kelly, L.; Shi, Y.; Huang, K.; Knerr, P. J.; Joewono, I.; Rusch, D.; Chisholm, S. W.; van der Donk, W. A. Catalytic promiscuity in the biosynthesis of cyclic peptide secondary metabolites in planktonic marine cyanobacteria *Proc. Natl. Acad. Sci. U.S.A.* **2010**, *107*, 10430.
(2) Shi, Y.; Yang, X.; Garg, N.; van der Donk, W. A. Production of lantipeptides in *Escherichia coli J. Am. Chem. Soc.* **2011**, *133*, 2338.
(3) Brademan, D. R.; Riley, N. M.; Kwiecien, N. W.; Coon, J. J. Interactive Peptide Spectral Annotator: A Versatile Web-based Tool for Proteomic Applications* *Molecular & Cellular Proteomics* **2019**, *18*, S193.
(4) Fernandez-Lima, F. A.; Kaplan, D. A.; Suetering, J.; Park, M. A. Gas-phase separation using a Trapped Ion Mobility Spectrometer *Int. J. Ion Mobil. Spectrom.* **2011**, *14*, 93.
(5) Fernandez-Lima, F. A.; Kaplan, D. A.; Park, M. A. Note: Integration of trapped ion mobility spectrometry with mass spectrometry *Rev. Sci. Instrum.* **2011**, *82*, 126106.
(6) Hernandez, D. R.; Debord, J. D.; Ridgeway, M. E.; Kaplan, D. A.; Park, M. A.; Fernandez-Lima, F. Ion dynamics in a trapped ion mobility spectrometer *Analyst* **2014**, *139*, 1913.
(7) Ridgeway, M. E.; Lubeck, M.; Jordens, J.; Mann, M.; Park, M. A. Trapped ion mobility spectrometry: A short review *Int. J. Mass Spectrom.* **2018**, *425*, 22.
(8) Silveira, J. A.; Michelmann, K.; Ridgeway, M. E.; Park, M. A. Fundamentals of Trapped Ion Mobility Spectrometry Part II: Fluid Dynamics *J. Am. Soc. Mass Spectrom.* **2016**, *27*, 585.
(9) Michelmann, K.; Silveira, J. A.; Ridgeway, M. E.; Park, M. A. Fundamentals of trapped ion mobility spectrometry *J. Am. Soc. Mass Spectrom.* **2015**, *26*, 14.
(10) Case, D. A.; Ben-Shalom, I. Y.; Brozell, S. R.; Cerutti, D. S.; III, T. E. C.; Cruzeiro, V. W. D.; Darden, T. A.; Duke, R. E.; Ghoreishi, D.; Gilson, M. K.; Gohlke, H.; Goetz, A. W.; Greene, D.; Harris, R.; Homeyer, N.; Huang, Y.; Izadi, S.; Kovalenko, A.; Kurtzman, T.; Lee, T. S.; LeGrand, S.; Li, P.; Lin, C.; Liu, J.; Luchko, T.; Luo, R.; Mermelstein, D. J.; Merz, K. M.; Miao, Y.; Monard, G.; Nguyen, C.; Nguyen, H.; Omelyan, I.; Onufriev, A.; Pan, F.; Qi, R.; Roe, D. R.; Roitberg, A.; Sagui, C.; Schott-Verdugo, S.; Shen, J.; Simmerling, C. L.; Smith, J.; SalomonFerrer, R.; Swails, J.; Walker, R. C.; Wang, J.; Wei, H.; Wolf, R. M.; Wu, X.; Xiao, L.; York, D. M.; Kollman, P. A. AMBER 2018. 2018, University of California, San Francisco
(11) Maier, J. A.; Martinez, C.; Kasavajhala, K.; Wickstrom, L.; Hauser, K. E.; Simmerling, C. ff14SB: Improving the Accuracy of Protein Side Chain and Backbone Parameters from ff99SB *J. Chem. Theory Comput.* **2015**, *11*, 3696.
(12) Wang, J.; Wolf, R. M.; Caldwell, J. W.; Kollman, P. A.; Case, D. A. Development and testing of a general amber force field *J. Comput. Chem.* **2004**, *25*, 1157.
(13) Bayly, C. I.; Cieplak, P.; Cornell, W. D.; Kollman, P. A. A well-behaved electrostatic potential based method using charge restraints for deriving atomic charges: the RESP model *J. Phys. Chem.* **1993**, *97*, 10269.
(14) Frisch, M. J.; Trucks, G. W.; Schlegel, H. B.; Scuseria, G. E.; Robb, M. A.; Cheeseman, J. R.; Scalmani, G.; Barone, V.; Petersson, G. A.; Nakatsuji, H.; Li, X.; Caricato, M.; Marenich, A. V.; Bloino, J.; Janesko, B. G.; Gomperts, R.; Mennucci, B.; Hratchian, H. P.; Ortiz, J. V.; Izmaylov, A. F.; Sonnenberg, J. L.; Williams-Young, D.; F. Ding; Lipparini, F.; F. Egidi; Goings, J.; Peng, B.; Petrone, A.; Henderson, T.; Ranasinghe, D.; Zakrzewski, V. G.; Gao, J.; Rega, N.; Zheng, G.; Liang, W.; Hada, M.; Ehara, M.; Toyota, K.; Fukuda, R.; Hasegawa, J.; Ishida, M.; Nakajima, T.; Honda, Y.; Kitao, O.; Nakai, H.; Vreven, T.; Throssell, K.; Jr., J. A. M.; Peralta, J. E.; Ogliaro, F.; Bearpark, M. J.; Heyd, J. J.; Brothers, E. N.; Kudin, K. N.; Staroverov, V. N.; Keith, T. A.; Kobayashi, R.; Normand, J.; Raghavachari, K.; Rendell, A. P.;

Burant, J. C.; Iyengar, S. S.; Tomasi, J.; Cossi, M.; Millam, J. M.; Klene, M.; Adamo, C.; Cammi, R.; Ochterski, J. W.; Martin, R. L.; Morokuma, K.; Farkas, O.; Foresman, J. B.; Fox, D. J. Gaussian 16, Revision C.01. 2016, Gaussian, Inc, Wallingford CT
(15) Jorgensen, W. L.; Chandrasekhar, J.; Madura, J. D.; Impey, R. W.; Klein, M. L. Comparison of Simple Potential Functions for Simulating Liquid Water *J. Chem. Phys.* **1983**, *79*, 926.
(16) Andersen, H. C. Molecular dynamics simulations at constant pressure and/or temperature *J. Chem. Phys.* **1980**, *72*, 2384.
(17) Andrea, T. A.; Swope, W. C.; Andersen, H. C. The role of long ranged forces in determining the structure and properties of liquid water *J. Chem. Phys.* **1983**, *79*, 4576.
(18) Miyamoto, S.; Kollman, P. A. Settle: An analytical version of the SHAKE and RATTLE algorithm for rigid water models *J. Comput. Chem.* **1992**, *13*, 952.
(19) Darden, T.; York, D.; Pedersen, L. Particle mesh Ewald: An *N*-log(N) method for Ewald sums in large systems *J. Chem. Phys.* **1993**, *98*, 10089.
(20) Onufriev, A.; Bashford, D.; Case, D. A. Exploring protein native states and large-scale conformational changes with a modified generalized born model *Proteins* **2004**, *55*, 383.
(21) Yu, Y.; Mukherjee, S.; van der Donk, W. A. Product formation by the promiscuous lanthipeptide synthetase ProcM is under kinetic control *J. Am. Chem. Soc.* **2015**, *137*, 5140.
(22) Walker, M. C.; Eslami, S. M.; Hetrick, K. J.; Ackenhusen, S. E.; Mitchell, D. A.; van der Donk, W. A. Precursor peptide-targeted mining of more than one hundred thousand genomes expands the lanthipeptide natural product family *BMC Genomics* **2020**, *21*, 387.
(23) Zimmermann, N.; Jung, G. The three-dimensional solution structure of the lantibiotic murein-biosynthesis-inhibitor actagardine determined by NMR *Eur. J. Biochem.* **1997**, *246*, 809.
(24) Xin, B.; Zheng, J.; Liu, H.; Li, J.; Ruan, L.; Peng, D.; Sajid, M.; Sun, M. Thusin, a Novel Two-Component Lantibiotic with Potent Antimicrobial Activity against Several Gram-Positive Pathogens *Frontiers Microbiol.* **2016**, *7*, 1115.
(25) Repka, L. M.; Chekan, J. R.; Nair, S. K.; van der Donk, W. A. Mechanistic Understanding of Lanthipeptide Biosynthetic Enzymes *Chem. Rev.* **2017**, *117*, 5457.
(26) Agrawal, P.; Khater, S.; Gupta, M.; Sain, N.; Mohanty, D. RiPPMiner: a bioinformatics resource for deciphering chemical structures of RiPPs based on prediction of cleavage and cross-links *Nucleic Acids Res.* **2017**, *45*, W80.
(27) Wang, J.; Zhang, L.; Teng, K.; Sun, S.; Sun, Z.; Zhong, J. Cerecidins, novel lantibiotics from Bacillus cereus with potent antimicrobial activity *Appl. Environ. Microbiol.* **2014**, *80*, 2633.
(28) Zhang, Q.; Yu, Y.; Vélasquez, J. E.; van der Donk, W. A. Evolution of lanthipeptide synthetases *Proc. Natl. Acad. Sci. USA* **2012**, *109*, 18361.
(29) Tang, W.; Jiménez-Osés, G.; Houk, K. N.; van der Donk, W. A. Substrate control in stereoselective lanthionine biosynthesis *Nat. Chem.* **2014**, *7*, 57.
(30) de Miguel, A.; Tapia-Rojo, R.; Utesch, T.; Mroginski, M. A. Structure, dynamics and kinetics of two-component Lantibiotic Lichenicidin *PLOS ONE* **2017**, *12*, e0179962.
(31) Wiedemann, I.; Böttiger, T.; Bonelli, R. R.; Schneider, T.; Sahl, H.-G.; Martínez, B. Lipid II-Based Antimicrobial Activity of the Lantibiotic Plantaricin C *Appl. Environ. Microbiol. y* **2006**, *72*, 2809.
(32) Tang, W.; van der Donk, W. A. Structural characterization of four prochlorosins: a novel class of lantipeptides produced by planktonic marine cyanobacteria *Biochemistry* **2012**, *51*, 4271.
(33) Geng, M.; Austin, F.; Shin, R.; Smith, L.; Elliot, M. A. Covalent Structure and Bioactivity of the Type AII Lantibiotic Salivaricin A2 *Appl. Environ. Microbiol.* **2018**, *84*, e02528.
(34) Barbour, A.; Wescombe, P.; Smith, L. Evolution of lantibiotic salivaricins: New weapons to fight infectious diseases *Trends Microbiol.* **2020**, *28*, 578.